ISSN 2096-7071
CN 10-1629/R1

# CHINA CDC WEEKLY

Vol. 5 No. 3 Jan. 20, 2023

# CCDC weekly

中国疾病预防控制中心周报

## Preplanned Studies



## Review



## Key Statistics



ISSN 2096-7071
9 772096 707231 0 3>

Cover photo: *Amanita exitialis* and *A. rimosa*, the top two lethal mushrooms killing the most people in China, 2022.

Preplanned Studies

# Mushroom Poisoning Outbreaks — China, 2022

Haijiao Li[1]; Yizhe Zhang[1]; Hongshun Zhang[1]; Jing Zhou[1]; Jiaqi Liang[1]; Yu Yin[1]; Qian He[1]; Shaofeng Jiang[1]; Yutao Zhang[1]; Yuan Yuan[1]; Nan Lang[1]; Bowen Cheng[1]; Mei Wang[1]; Chengye Sun[1,#]

**Summary**

**What is already known about this topic?**

Mushroom poisoning is one of the most serious food safety issues in China. By the end of 2021, over 520 poisonous mushrooms had been discovered in China. The Southwest region of China was the most severely affected. Mushroom poisonings mainly concentrated in the summer and autumn months.

**What is added by this report?**

In 2022, China CDC conducted an investigation of 482 incidents of mushroom poisoning across 21 provincial-level administrative divisions (PLADs). This resulted in 1,332 patients and 28 deaths, with a total case fatality rate of 2.1%. A total of 98 mushrooms were identified, causing 7 different clinical types of diseases. Three provisional new species (*Collybia humida* nom. prov., *Spodocybe venenata* nom. prov., and *Omphalotus yunnanensis* nom. prov.) were newly recorded as poisonous mushrooms in China, in addition to 10 other species.

**What are the implications for public health practice?**

In view of the extensive impact and harm of poisonous mushrooms on public health, it is necessary to promote prevention and improve the ability of professionals to identify, diagnose, and treat mushroom poisoning.

Mushroom poisoning has become a serious food safety issue in China. With the support of the government, over the past decade, China has gradually established a mushroom poisoning prevention and treatment system involving experts in disease prevention and control, clinical diagnosis and treatment, fungal classification, and basic medicine (*1*–*3*). In recent years, a mushroom-poisoning information collecting, diagnosis, and treatment support network has been established, utilizing WeChat, telephone, email, and other methods. After poisoning incidents occur, mushroom samples are collected by CDC staff or hospital professionals and sent to mycological researchers at universities and institutions for identification, based on morphological characters and DNA sequence data (*1*–*3*).

In 2022, China CDC investigated 482 mushroom poisoning incidents involving 1,332 patients and 28 deaths, with a total case fatality rate of 2.1%. The number of cases per incident ranged from 1 to 28, with an average of 2. A total of 13 incidents involved more than 10 patients. Of these cases, 73 patients from 23 incidents ate poisonous mushrooms purchased from markets or given by friends; 9 patients from 6 incidents were poisoned after eating raw *Chlorophyllum molybdites*, *Boletus bainiugan*, and *Macrocybe gigantea*, although the last two species were considered to be edible after proper cooking (Supplementary Table S1, available in https://weekly.chinacdc.cn/); 44 patients from 7 incidents were poisoned after eating dried mushrooms; and 213 patients and 3 deaths from 55 incidents ate mixed mushrooms.

The temporal distribution shows that mushroom poisonings occurred in all months, with the highest number of incidents occurring between May and November (460 incidents, 1,234 patients, and 22 deaths). The first death occurred in mid-February in Fujian. The top 3 months for deaths were June (13 deaths), July (3 deaths), and September (3 deaths) (Figure 1).

In terms of geographical distribution, mushroom poisoning incidents were reported in 21 provincial-level administrative divisions (PLADs). Overall, 10 PLADs had more than 10 incidents, and Yunnan, Hunan, Sichuan, Guangxi, Chongqing, and Zhejiang were the top 6 (Table 1); 11 PLADs had more than 20 patients, and Yunnan, Hunan, Sichuan, and Guangxi had over 100 patients each (Table 1). Yunnan, Hunan, and Guangdong were the top 3 PLADs in terms of deaths, with 9, 7, and 5 deaths, respectively (Table 1). Southwest China (Yunnan, Sichuan, Chongqing, and Guizhou) was the most severely affected region, with 234 incidents, 703 patients, and 13 deaths. This was followed by Central China (Hunan, Hubei, and Henan) with 109 incidents, 277 patients, and 8 deaths; East China (Zhejiang, Fujian, Jiangsu, Jiangxi, Anhui,

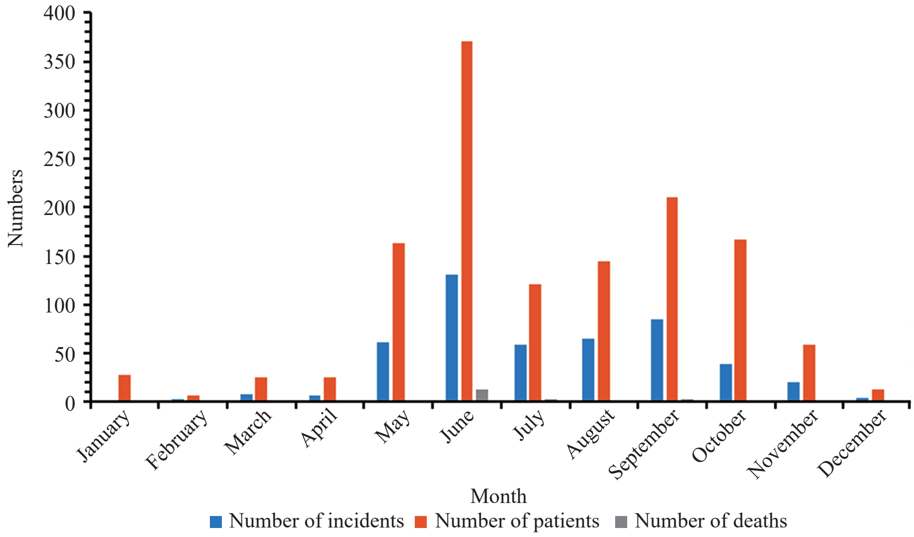


FIGURE 1. Monthly distribution of mushroom poisonings in China, 2022.

TABLE 1. Geographical distribution of mushroom poisoning incidents in China, 2022.

| PLAD | Number of incidents | Number of patients | Deaths | Mortality (%) |
|---|---|---|---|---|
| Yunnan | 131 | 404 | 9 | 2.23 |
| Hunan | 89 | 229 | 7 | 3.06 |
| Sichuan | 57 | 130 | 2 | 1.54 |
| Guangxi | 29 | 106 | 0 | 0 |
| Chongqing | 27 | 82 | 1 | 1.22 |
| Zhejiang | 27 | 72 | 0 | 0 |
| Guangdong | 20 | 46 | 5 | 10.87 |
| Guizhou | 19 | 87 | 1 | 1.15 |
| Ningxia | 19 | 29 | 0 | 0 |
| Hubei | 17 | 42 | 0 | 0 |
| Shandong | 9 | 19 | 1 | 5.26 |
| Fujian | 8 | 15 | 1 | 6.67 |
| Jiangsu | 7 | 20 | 0 | 0 |
| Jiangxi | 6 | 7 | 0 | 0 |
| Anhui | 5 | 16 | 0 | 0 |
| Hebei | 4 | 10 | 0 | 0 |
| Henan | 3 | 6 | 1 | 16.67 |
| Shanghai | 2 | 2 | 0 | 0 |
| Liaoning | 1 | 5 | 0 | 0 |
| Shanxi | 1 | 3 | 0 | 0 |
| Heilongjiang | 1 | 2 | 0 | 0 |
| Total | 482 | 1,332 | 28 | 2.10 |

Note: Species newly recorded as poisonous mushrooms in China are in italic bold.
Abbreviation: ALF=Acute liver failure; ARF=Acute renal failure; G=Gastroenteritis; P=Psycho to neurological disorder; M=Medicinal; U=Unclassified; E=edible.

and Shanghai) with 55 incidents, 132 patients, and 1 death; South China (Guangxi and Guangdong) with 49 incidents, 152 patients, and 5 deaths; Northwest China (Ningxia) with 19 incidents, 29 patients, and 0 deaths; North China (Shandong, Hebei, and Shanxi) with 14 incidents, 32 patients, and 1 death; and Northeast China (Liaoning and Heilongjiang) with 2 incidents, 7 patients, and 0 deaths. Detailed information for each PLAD is presented in Table 1.

In 2022, 98 species of poisonous mushrooms were successfully identified from mushroom poisoning events, resulting in seven different clinical syndromes. Among these 98 species, 13 were newly recorded as poisonous species in China. *Collybia humida* nom. prov.*,* *Spodocybe venenata* nom. prov., and *Omphalotus yunnanensis* nom. prov. represented 3 undescribed species. The first two species contained muscarine and stimulated the parasympathetic nervous system, while the last species caused gastroenteritis. *Coprinopsis aesontiensis* and *Leucoagaricus purpureolilacinus* species complex were two new records in China causing gastroenteritis. The eight remaining species, previously of unclear edibility, were confirmed to be poisonous based on poisoning incidents. These species were *Tricholoma olivaceum*, a species originally discovered in China and causing gastroenteritis (*4*); *Candolleomyces yanshanensis*, *Anthracoporus holophaeus*, *Anthracoporus nigropurpureus*, *Inocybe* cf. *assimillata*, *Inocybe* aff. *decemgibbosa*, *Inocybe* aff. *pseudoreducta,* and *Inosperma* cf. *gregarium,* which caused psycho-neurological disorders (*5*–*6*).

The top three lethal mushroom species were *Amanita exitialis*, *A. rimosa,* and *Russula subnigricans*, which caused 7, 7, and 6 deaths, respectively (Figure 2, Supplementary Table S1). *Chlorophyllum molybdites*, the most widely distributed mushroom (discovered in 16 PLADs), caused the most poisonings incidents (appearing in 114 incidents and affecting 257 patients) and had a distinct long active period (from early April to early December).

In 2022, nine species causing acute liver failure were identified in China (Figure 2, Supplementary Table S1). *Amanita exitialis* was the most dangerous species, causing 7 deaths in 14 incidents involving 41 patients. *Amanita rimosa* and *Galerina sulciceps* caused seven and three deaths, respectively. *Amanita subfuliginea*, a lethal species originally described from Guangdong in 2016 (*7*), was also identified. On May 29, two people from Chongqing were poisoned by a gray amanita mushroom, marking the first reported poisoning incident since the mushroom was described and the first record of this gray poisonous amanita in Southwest China (*7*).

Three species of mushroom were identified as causing acute renal failure in mushroom poisoning incidents (Figure 2, Supplementary Table S1). *Amanita pseudoporphyria* was the most common, appearing in 12 incidents either alone or in combination with other species. *Amanita neoovoidea* had the longest active period, occurring from mid-June to early November.

*Russula subnigricans* was linked to 15 incidents of rhabdomyolysis, involving 44 patients and resulting in 6 deaths, either alone or in combination with other mushroom species. This species was found in Yunnan, Hunan, and Zhejiang from June to September. The first *Paxillus orientalis* poisoning incident from China, resulting in hemolysis, occurred in Sichuan in early June (Figure 2, Supplementary Table S1).

A total of 51 species causing gastroenteritis were identified from mushroom poisoning incidents in China in 2022 (Supplementary Table S1). Among them, four species were identified as poisonous mushrooms and subsequently added to the Chinese poisonous mushroom list (*1*–*3*,*8*). *Omphalotus yunnanensis* nom. prov. was discovered from a poisoning incident in Yunnan. The top three species in this category were *Chlorophyllum molybdites*, *Russula japonica,* and *Scleroderma cepa* (Figure 2).

In 2022, 32 species of mushrooms causing psycho-neurological disorders were identified in China (Supplementary Table S1). Nine of these species were newly discovered as poisonous (*1*–*3*,*8*), including *Collybia humida* nom. prov. and *Spodocybe venenata* nom. prov., which need to be formally described. The top five species were *Lanmaoa asiatica*, *Gymnopilus dilepis*, *Anthracoporus nigropurpureus*, *Amanita rufoferruginea*, and *Amanita sychnopyramis* f. *subannulata* (Figure 2).

On September 30, five Burmese workers in Dehong, Yunnan were poisoned by *Inosperma hainanense*, a newly discovered species containing muscarine that was identified in Hainan in 2021 (*9*).

## DISCUSSION

In 2022, mushroom poisoning incidents and patients were more than those in 2019 and 2021 but fewer than in 2020, while deaths slightly increased (28 compared to 22, 20, and 25) (*1*–*3*). Heilongjiang was newly recorded with poisoning incidents (*1*–*3*). A total of 98 poisonous species were successfully identified from poisoning incidents in 2022, among which 62 species had already been recorded from 2019 to 2021 (*1*–*3*), raising the total number of species from incidents to over 190 in China by the end of 2022.

FIGURE 2. Poisonous mushrooms identified from mushroom poisoning incidents in China in 2022.
Note: 1: *Amanita exitialis*; 2: *A. fuliginea*; 3: *A. fuligineoides*; 4: *A. rimosa*; 5: *A. subfuliginea* (provided by Yalin Zhou); 6: *A. subjunquillea*; 7: *A. pallidorosea*; 8: *Galerina sulciceps*; 9: *Lepiota brunneoincarnata*; 10: *Russula subnigricans*; 11: *A. neoovoidea*; 12: *A. oberwinklerana*; 13: *A. pseudoporphyria*; 14: *Paxillus orientalis*; 15: *Cordierites frondosus*; 16: *Chlorophyllum molybdites*; 17: *Russula japonica*; 18: *Scleroderma cepa* (provided by Tianhong Li); 19: *Coprinopsis aesontiensis* (provided by Wensong Chen); 20: *Leucoagaricus purpureolilacinus* species complex (provided by Xia Rong); 21: *Omphalotus yunnanensis* nom. prov.; 22: *Tricholoma olivaceum*; 23: *Lanmaoa asiatica* (provided by Guanliang Wen); 24: *Gymnopilus dilepis* (provided by Ya'an CDC); 25: *Anthracoporus nigropurpureus*; 26: *Amanita rufoferruginea*; 27: *A. sychnopyramis* f. *subannulata* (provided by Zuohong Chen); 28: *Anthracoporus holophaeus* (provided by Yanchun Li); 29: *Collybia humida* nom. prov.; 30: *Spodocybe venenata* nom. prov.

The most dangerous mushrooms were *Amanita exitialis* and *A. rimosa*, each causing seven deaths in 2022, different from 2019 to 2021 (*1*–*3*).

Temporal distribution analysis showed that mushroom poisonings in 2022 were concentrated from May to November, similar to 2021 but longer than 2019 and 2020 (*1*–*3*). The peak occurred in June and the incidents decreased in July and August, likely due to the rare drought in southern China. With the arrival of rain in September, mushroom poisoning reached its second peak in September and then gradually decreased in the following three months (Figure 1).

From 2019 to 2021, Hunan was the province with the most incidents among PLADs. However, in 2022, Yunnan had the highest number of incidents, and Southwest China remained the most severely affected area (*1–3*). Yunnan also had the most deaths over the last four years (*1–3*).

On June 5, one person in Sichuan was poisoned by *Paxillus orientalis*, resulting in hemolysis. This was the first reported case of poisoning from this species in China (*10*). In 2020 and 2021, species of the same genus, *Paxillus involutus*, were reported to have caused poisoning in Xizang (Tibet) and Inner Mongolia (*2–3*). We strongly advise against collecting and eating species of *Paxillus*, despite their previous acceptance as edible and/or medicinal fungi in China and the perception of safety among many people (*8*,*10*).

In 2022, 51 species of gastroenteritis-causing organisms were identified, more than in 2019 (30 species) and 2021 (39 species), but slightly fewer than in 2020 (56 species). The top two species were *Chlorophyllum molybdites* and *Russula japonica*, which remained the same from 2019 to 2021, but the third species in 2022 was *Scleroderma cepa*, instead of *Entoloma omiense* in the previous three years (*1–3*).

In 2022, 32 species causing psycho-neurological disorders were identified, more than the 18, 28, and 22 species reported in the previous three years (*1–3*). Surprisingly, *Lanmaoa asiatica* ranked first, unlike the previous three years when *Amanita subglobosa* was the most common (*1–3*). *Lanmaoa asiatica* is a delicious bolete that must be cooked properly (*8*). The increased poisoning incidents of this species may be partially attributed to the rise of online shopping, which lacks face-to-face communication about proper cooking.

*Anthracoporus nigropurpureus* (*Porphyrellus nigropurpureus*), a black bolete, caused nine poisoning incidents in Sichuan, Yunnan, and Zhejiang, resulting in dizziness, blurred vision, amyosthenia, headache, muscle cramps, hand or foot tremors, and red eyes, among other symptoms. However, its toxicity remains unclear, and further studies are urgently needed. Another species from the same genus, *Anthracoporus holophaeus*, was also identified from two incidents with similar clinical manifestations. At present, we strongly advise against collecting and eating black boletes of the genus *Anthracoporus*.

*Cordierites frondosus* is a species morphologically similar to edible *Auricularia* spp., but the former species can cause typical photosensitive dermatitis, which poisoned three people from Chongqing on April 21, 2022. Compared to 2019, we found that this species appeared in different months in different areas; for example, two incidents occurred in Yunnan in early June and in Guizhou in early December (*1*). Further research is needed to uncover its spatial and temporal distribution characteristics and rules for better poisoning control.

Sixteen edible mushrooms were identified from mushroom poisoning incidents in 2022 (Supplementary Table S1). These incidents were likely due to the consumption of mixed mushrooms with poisonous mushrooms, contaminated mushrooms, or some species that may be poisonous to certain individuals.

This study only represents a portion of actual mushroom poisonings. In some cases, no mushroom specimens were obtained, making it impossible to confirm the exact poisonous mushroom species. To reduce the risk of poisoning, we recommend that people set aside some fruiting bodies before eating or take a photo of the fresh mushrooms before cooking. Knowledge popularization of poisonous mushrooms is also important to decrease the number of poisoning incidents. To this end, we recommend creating more scientific, plain, and varied popularization materials and publicizing them to people at risk before and throughout the poisoning season. In the past decades, our knowledge of poisonous mushrooms has increased drastically, and more patient poisoning incidents have become more standardized.

The previous practice of controlling and preventing mushroom poisoning demonstrates that more effort and closer cooperation are urgently needed from governments, CDC staff, doctors, and mycologists in the future.

**Acknowledgements**: Profs. Zuohong Chen, Ping Zhang (Hunan Normal University), Prof. Zhuliang Yang, Drs. Xianghua Wang, Gang Wu, Hong Luo, Zaiwei Ge, Yanchun Li (Kunming Institute of Botany, Chinese Academy of Sciences), Profs. Taihui Li, Wangqiu Deng, Drs. Ming Zhang, Chaoqun Wang (Institute of Microbiology, Guangdong Academy of Sciences), Prof. Tolgor Bau (Jilin Agricultural University), Drs. Niankai Zeng, Yuguang Fan (Hainan Medical University), Prof. Liping Tang (Kunming Medical University), Prof. Junfeng Liang, Dr. Jie Song (Research Institute of Tropical Forestry, Chinese Academy of Forestry), Profs. Yucheng Dai, Baokai Cui, Shuanghui He, Dr. Jing Si (Beijing Forestry University), Dr. Chuanhua Li (Shanghai Academy of Agricultural Sciences), Prof. Haisheng Yuan (Institute of Applied Ecology, Chinese Academy of Sciences), Dr. Xiaolan He (Institute of Agricultural Resources and Environment, Sichuan Academy of Agricultural Science) and Profs. Liangdong Guo, Lei Cai, Ruilin Zhao, Xiaoyong Liu (Institute of Microbiology, Chinese Academy of Sciences); involved CDCs and hospitals.

**Funding:** The research was financed by the National Natural Science Foundation of China (32270021).

**doi:** 10.46234/ccdcw2023.009

# Corresponding author: Chengye Sun, suncy@chinacdc.cn.

[1] National Institute of Occupational Health and Poison Control, Chinese Center for Disease Control and Prevention, Beijing, China.

Submitted: January 07, 2023; Accepted: January 16, 2023

## REFERENCES

1. Li HJ, Zhang HS, Zhang YZ, Zhang KP, Zhou J, Yin Y, et al. Mushroom poisoning outbreaks — China, 2019. China CDC Wkly 2020;2(2):19 – 24. http://dx.doi.org/10.46234/ccdcw2020.005.
2. Li HJ, Zhang HS, Zhang YZ, Zhou J, Yin Y, He Q, et al. Mushroom poisoning outbreaks — China, 2020. China CDC Wkly 2021;3(3):41 – 5. http://dx.doi.org/10.46234/ccdcw2021.014.
3. Li HJ, Zhang HS, Zhang YZ, Zhou J, Yin Y, He Q, et al. Mushroom poisoning outbreaks — China, 2021. China CDC Wkly 2022;4(3):35 – 40. http://dx.doi.org/10.46234/ccdcw2022.010.
4. Reschke K, Popa F, Yang ZL, Kost G. Diversity and taxonomy of *Tricholoma* species from Yunnan, China, and notes on species from Europe and North America. Mycologia 2018;110(6):1081 – 109. http://dx.doi.org/10.1080/00275514.2018.1512295.
5. Zhou H, Cheng GQ, Sun XM, Cheng RY, Zhang HL, Dong YM, et al. Three new species of *Candolleomyces* (Agaricomycetes, Agaricales, Psathyrellaceae) from the Yanshan Mountains in China. MycoKeys 2022;88:109 – 21. http://dx.doi.org/10.3897/mycokeys.88.81437.
6. Li YC, Yang ZL. The boletes of China: *Tylopilus* s.l. Singapore: Springer. 2021. http://dx.doi.org/10.1007/978-981-16-2986-0.
7. Cai Q, Cui YY, Yang ZL. Lethal *Amanita* species in China. Mycologia 2016;108(5):993 – 1009. http://dx.doi.org/10.3852/16-008.
8. Wu F, Zhou LW, Yang ZL, Bau T, Li TH, Dai YC. Resource diversity of Chinese macrofungi: edible, medicinal and poisonous species. Fungal Divers 2019;98(1):1 – 76. http://dx.doi.org/10.1007/s13225-019-00432-7.
9. Deng LS, Kang R, Zeng NK, Yu WJ, Chang C, Xu F, et al. Two new *Inosperma* (Inocybaceae) species with unexpected muscarine contents from tropical China. MycoKeys 2021;85:87 – 108. http://dx.doi.org/10.3897/mycokeys.85.71957.
10. White J, Weinstein SA, De Haro L, Bédry R, Schaper A, Rumack BH, et al. Mushroom poisoning: a proposed new clinical classification. Toxicon 2019;157:53 – 65. http://dx.doi.org/10.1016/j.toxicon.2018.11.007.

# SUPPLEMENTARY MATERIAL

SUPPLEMENTARY TABLE S1. Mushroom species involved in poisoning incidents and their spatial and temporal distribution in China, 2022.

| Mushroom species | Number of incidents | Number of patients | Deaths | Case fatality (%) | Spatial and temporal distribution |
|---|---|---|---|---|---|
| Acute liver failure | | | | | |
| *Amanita exitialis* | 14 | 41 | 7 | 17.07 | February 13 to April 1, Fujian and Guangdong; May 6 to 30, Sichuan and Guizhou; June 7 to July 2, Yunnan |
| *Amanita* cf. *exitialis* | 1 | 1 | 0 | 0.00 | May 29, Guangxi |
| *Amanita fuliginea* | 8 | 19 | 0 | 0.00 | May 23 to June 19, Hunan |
| *Amanita fuliginea*, *A. fritillaria*[P] and *Russula* spp.[U] | 1 | 1 | 0 | 0.00 | June 13, Hunan |
| *Amanita fuligineoides* | 1 | 4 | 0 | 0.00 | June 8, Yunnan |
| *Amanita fuligineoides*, *A. pseudoporphyria*[ARF] and *A. kitamagotake*[E] | 1 | 2 | 0 | 0.00 | June 15, Zhejiang |
| *Amanita* cf. *pallidorosea* | 2 | 5 | 1 | 20.00 | July 28, Henan; September 1, Shandong |
| *Amanita rimosa* | 4 | 27 | 7 | 25.93 | June 11 to 25, Hunan, Zhejiang |
| *Amanita subfuliginea* | 1 | 2 | 0 | 0.00 | May 29, Chongqing |
| *Amanita subjunquillea* | 3 | 9 | 0 | 0.00 | June 11 and 24, Guizhou; September 1, Shandong |
| *Amanita subjunquillea*, *A. fritillaria*[P], *Lactarius oomsisiensis*[G] and *Agaricus flocculosipes*[E] | 1 | 2 | 0 | 0.00 | July 27, Shandong |
| *Amanita subjunquillea*, *Amanita pallidorosea*[ALF], *Amanita oberwinklerana*[ARF], *Hypholoma fasciculare*[G], *Agaricus abruptibulbus*[G], *Agaricus sinoplacomyces*[G], *Amanita fritillaria*[P], *Agaricus flocculosipes*[E], *Lepista nuda*[E], *Agaricus beijingensis*[U] and *Lanmaoa* sp.[U] | 1 | 5 | 0 | 0.00 | September 23, Liaoning (bought from market) |
| *Amanita* sp., *Suillus luteus*[G], *Lactarius hatsudake*[E] and *Russula sanguinea*[E] | 1 | 2 | 1 | 50.00 | September 1, Shandong |
| *Amanita* sp. | 1 | 5 | 1 | 20.00 | May 19, Chongqing |
| *Galerina sulciceps* | 9 | 33 | 3 | 9.09 | June 19, Guizhou; September 22 to November 26, Sichuan, Yunnan, Guizhou |
| *Galerina* sp. | 1 | 1 | 0 | 0.00 | June 19, Yunnan |
| *Lepiota brunneoincarnata* | 11 | 17 | 0 | 0.00 | June 27, Ningxia; July 5, Yunnan; July 15 to August 28, Ningxia |
| Rhabdomyolysis | | | | | |
| *Russula subnigricans* | 11 | 32 | 6 | 18.75 | June 22 to September 23, Yunnan, Hunan |
| *Russula subnigricans* and *R. adusta*[E] | 2 | 3 | 0 | 0.00 | August 18 and September 5, Yunnan |
| *Russula subnigricans*, *R.* cf. *nigricans*[E] and *R. densifolia*[E] | 1 | 7 | 0 | 0.00 | July 23, Zhejiang |
| *Russula subnigricans*, *Lactifluus sinensis*[E], *Russula pseudocompacta*[E], *Russula viridirubrolimbata*[E], *Xerocomus parvulus*[E] and *Russula* sp.[U] | 1 | 2 | 0 | 0.00 | July 10, Hunan (bought from market) |
| Acute renal failure | | | | | |
| *Amanita neoovoidea* | 4 | 6 | 0 | 0.00 | June 16, Yunnan; September 19 to October 1, Zhejiang; November 4, Chongqing (bought from market) |
| *Amanita oberwinklerana* | 5 | 11 | 0 | 0.00 | June 23 to July 1, Guizhou and Yunnan; August 1, Jiangsu; August 31, Hebei |
| *Amanita* cf. *oberwinklerana* | 1 | 3 | 0 | 0.00 | August 13, Hebei |
| *Amanita pseudoporphyria* | 9 | 20 | 0 | 0.00 | May 25 to July 6, Guangxi, Jiangxi, Hubei, Hunan, Yunnan |
| *Amanita pseudoporphyria* and *Russula japonica*[G] | 2 | 6 | 0 | 0.00 | June 13 and 14, Zhejiang, Hunan |
| *Amanita pseudoporphyria* and *A. fritillaria*[P] | 1 | 4 | 0 | 0.00 | June 14, Hunan |

Continued

| Mushroom species | Number of incidents | Number of patients | Deaths | Case fatality (%) | Spatial and temporal distribution |
|---|---|---|---|---|---|
| Hemolysis | | | | | |
| *Paxillus orientalis* | 1 | 1 | 0 | 0.00 | June 5, Sichuan |
| Gastroenteritis | | | | | |
| *Agaricus bresadolanus* and *Lycoperdon pratense*[E] | 1 | 2 | 0 | 0.00 | August 25, Shandong |
| *Albatrellus dispansus* | 1 | 1 | 0 | 0.00 | August 1, Yunnan |
| *Baorangia major* | 2 | 9 | 0 | 0.00 | May 26 and 29, Yunnan (one incident bought from market) |
| *Chlorophyllum globosum* | 1 | 4 | 0 | 0.00 | May 31, Yunnan |
| *Chlorophyllum* aff. *globosum* | 3 | 10 | 0 | 0.00 | September 12 to 27, Sichuan |
| *Chlorophyllum hortense* | 1 | 1 | 0 | 0.00 | July 25, Hubei |
| *Chlorophyllum molybdites* | 114 | 257 | 0 | 0.00 | April 2 to December 6, Guangdong, Hubei, Jiangxi, Guangxi, Hunan, Fujian, Sichuan, Chongqing, Yunnan, Shandong, Anhui, Jiangsu, Sichuan, Zhejiang, Shanghai, Fujian (5 patients in 4 incidents from Guangdong, Shanghai and Jiangsu were eaten raw) |
| *Chlorophyllum* cf. *molybdites* | 1 | 1 | 0 | 0.00 | September 2, Henan |
| *Coprinopsis aesontiensis* | 1 | 6 | 0 | 0.00 | April 21, Yunnan |
| *Entoloma* cf. *sinuatum* | 1 | 2 | 0 | 0.00 | August 13, Yunnan |
| *Entoloma* sp., *Xerocomus parvulus*[E], *Russula* cf. *pseudobubalina*[U] | 1 | 2 | 0 | 0.00 | September 9, Zhejiang |
| *Entoloma omiense* | 5 | 15 | 0 | 0.00 | June 6, Yunnan; July 12 and August 13, Guangxi, Guangdong; September 14 and 21, Zhejiang, Guizhou |
| *Entoloma omiense*, *Suillus pinetorum*[G], *Suillus luteus*[G], *Amanita sinocitrina*[P], *Lycoperdon perlatum*[E,M] and *Lactarius vividus*[E] | 1 | 5 | 0 | 0.00 | September 24, Sichuan |
| *Gymnopus densilamellatus* | 1 | 3 | 0 | 0.00 | May 30, Yunnan (bought from market) |
| *Gymnopus dryophilus* | 1 | 1 | 0 | 0.00 | June 15, Yunnan |
| *Heimioporus gaojiaocong* | 1 | 5 | 0 | 0.00 | August 24, Guizhou |
| *Lactarius hirtipes* | 1 | 2 | 0 | 0.00 | October 10, Sichuan |
| *Lactarius laccarioides* | 1 | 1 | 0 | 0.00 | August 7, Yunnan |
| *Lactarius rubrocorrugatus* | 1 | 1 | 0 | 0.00 | June 13, Yunnan |
| *Lactarius subhirtipes* or *L. subatlanticus*[G] | 1 | 1 | 0 | 0.00 | June 13, Chongqing |
| *Lactifluus pseudoluteopus* | 1 | 3 | 0 | 0.00 | June 14, Yunnan (bought from market) |
| *Lactifluus piperatus* | 1 | 5 | 0 | 0.00 | June 23, Yunnan |
| *Leucoagaricus leucothites* | 2 | 6 | 0 | 0.00 | September 21, Ningxia; November 27, Anhui |
| ***Leucoagaricus purpureolilacinus* species complex** | 1 | 1 | 0 | 0.00 | September 21, Sichuan |
| *Neoboletus venenatus* | 1 | 8 | 0 | 0.00 | August 2, Sichuan |
| *Neoboletus venenatus* and *Butyriboletus yicibus*[E] | 1 | 2 | 0 | 0.00 | Late June, Hunan (dried boletes, bought from market) |
| *Omphalotus guepiniformis* | 3 | 18 | 0 | 0.00 | March 25 and 26, Guangxi; December 13, Fujian |
| *Omphalotus guepiniformis* and *Macrolepiota procera*[E,M,G] | 1 | 8 | 0 | 0.00 | October 5, Yunnan |
| *Omphalotus olearius* | 1 | 3 | 0 | 0.00 | September 24, Yunnan |

Continued

| Mushroom species | Number of incidents | Number of patients | Deaths | Case fatality (%) | Spatial and temporal distribution |
|---|---|---|---|---|---|
| ***Omphalotus yunnanensis*** **nom. prov.** | 1 | 1 | 0 | 0.00 | September 24, Yunnan |
| *Rubroboletus latisporus* | 2 | 10 | 0 | 0.00 | July 22, Yunnan; October 2, Guizhou |
| *Russula japonica* | 42 | 136 | 0 | 0.00 | May 16 to October 27, Yunnan, Hunan, Chongqing, Sichuan, Zhejiang, Guizhou, Anhui |
| *Russula japonica*, *R. crustosa*[E,M] and *Amanita fritillaria*[P] | 1 | 1 | 0 | 0.00 | June 8, Hunan |
| *Russula japonica*, *Lactifluus volemus*[E] and *Hygrocybe* sp.[U] | 1 | 5 | 0 | 0.00 | June 8, Chongqing |
| *Russula japonica* and *R. aeruginea*[E] | 1 | 2 | 0 | 0.00 | June 10, Hunan |
| *Russula japonica* and *R. compacta*[E] | 1 | 4 | 0 | 0.00 | June 9, Hunan |
| *Russula japonica* and *R. punctipes*[G] | 1 | 2 | 0 | 0.00 | June 1, Hunan |
| *Russula japonica* and *R. punctipes*[G], *R. virescens*[E] and *Lactifluus leoninus*[E] | 1 | 3 | 0 | 0.00 | August 10, Sichuan |
| *Russula japonica*, *Suillus granulatus*[E,G] and *Tylopilus pseudoballoui*[E] | 1 | 1 | 0 | 0.00 | July 16, Yunnan |
| *Russula japonica* and *Gomphus* sp.[U] | 1 | 1 | 0 | 0.00 | July 11, Yunnan |
| *Russula japonica* and *Russula* sp.[U] | 1 | 2 | 0 | 0.00 | August 7, Sichuan |
| *Russula rufobasalis* | 1 | 3 | 0 | 0.00 | May 29, Hunan |
| *Scleroderma* aff. *albidum* | 1 | 2 | 0 | 0.00 | September 7, Yunnan |
| *Scleroderma* cf. *areolatum* and *Scleroderma yunnanense*[E] | 1 | 9 | 2 | 22.22 | June 12, Yunnan |
| *Scleroderma cepa* | 9 | 41 | 0 | 0.00 | June 20 to August 7, Yunnan; September 9 and 18, Yunnan, Hunan; October 25, Zhejiang |
| *Scleroderma cepa* and *S. bovista*[E,M] | 1 | 2 | 0 | 0.00 | June 17, Yunnan |
| *Scleroderma venenatum* | 1 | 2 | 0 | 0.00 | September 1, Hebei |
| *Suillus granulatus* and *Lactarius hatsudake*[E] | 1 | 1 | 0 | 0.00 | June 13, Chongqing |
| *Suillus phylopictus*, *Amanita vaginata* complex[U], *Lactarius cinnamomeus*[E], *Russula compacta*[E], *Cortinarius hinnuleoarmillatus*[U], *Veloporphyrellus pseudovelatus*[U], *Entoloma undatum*[U], *Lactarius brachycystidiatus*[U] and *Russula* spp.[U] | 1 | 2 | 0 | 0.00 | July 8, Yunnan |
| *Tricholoma equestre* and *Tricholoma* sp.[U] | 1 | 1 | 0 | 0.00 | October 10, Yunnan |
| *Thicholoma highlandense* and *Tricholoma* sp.[G] | 1 | 6 | 0 | 0.00 | October 6, Yunnan |
| *Tricholoma highlandense*, *Gomphus floccosus*[G], *Boletus* sp.[U], *Russula* spp.[U] and *Ramaria* sp.[U] | 1 | 4 | 0 | 0.00 | June 14, Yunnan |
| ***Tricholoma olivaceum*** | 1 | 2 | 0 | 0.00 | August 18, Yunnan |
| *Tricholoma stans*, *Hygrophorus yunnanensis*[E] and *Hygrophorus* sp.[U] | 1 | 6 | 0 | 0.00 | October 17, Guizhou (eaten in a restaurant) |
| *Tylopilus felleus*, *Suillus granulatus*[G,E], *Amanita fritillaria*[P], *Amanita* cf. *hemibapha*[E], *Amanita princeps*[E], *Russula cerolens*[U], *Russula* sp.[U], *Lactifluus* sp.[U] and *Cortinarius* sp.[U] | 1 | 2 | 0 | 0.00 | July 8, Shandong |
| **Psycho-neurological disorder** | | | | | |
| *Amanita concentrica* | 1 | 2 | 0 | 0.00 | June 15, Yunnan |
| *Amanita melleiceps* and *Gymnopus* sp.[U] | 1 | 2 | 0 | 0.00 | June 10, Fujian |
| *Amanita pseudosychnopyramis* | 1 | 1 | 0 | 0.00 | March 26, Zhejiang |
| *Amanita rufoferruginea* | 4 | 11 | 0 | 0.00 | June 10 to 14, Hunan, Chongqing, Guangxi; August 4, Sichuan |

Continued

| Mushroom species | Number of incidents | Number of patients | Deaths | Case fatality (%) | Spatial and temporal distribution |
|---|---|---|---|---|---|
| *Amanita rufoferruginea*, *Russula compacta*[E] and *Termitomyces* sp.[E] | 1 | 4 | 0 | 0.00 | June 9, Zhejiang |
| *Amanita rufoferruginea*, *A. subglobosa*[P] | 1 | 3 | 0 | 0.00 | June 17, Hunan |
| *Amanita subglobosa* | 2 | 4 | 0 | 0.00 | June 1 to July 29, Chongqing |
| *Amanita sychnopyramis* f. *subannulata* | 5 | 15 | 0 | 0.00 | May 18 to June 12, Guangxi, Hunan |
| ***Anthracoporus holophaeus*** | 1 | 1 | 0 | 0.00 | June 10, Yunnan |
| *Anthracoporus holophaeus*, *Lactarius subhirtipes*[G] | 1 | 3 | 0 | 0.00 | June 5, Sichuan |
| ***Anthracoporus nigropurpureus*** | 9 | 17 | 0 | 0.00 | June 10 to July 13, Sichuan, Yunnan, Zhejiang |
| ***Candolleomyces yanshanensis*** | 1 | 3 | 0 | 0.00 | June 16, Shandong |
| *Clitocybe nebularis* | 1 | 1 | 0 | 0.00 | August 25, Yunnan |
| ***Collybia humida* nom. prov.**, ***Spodocybe venenata* nom. prov.**[P], *Hypholoma fasciculare*[G], *Pholiota multicingulata*[G], *Gymnopus dryophilus*[G], *Lactarius citrinus*[G], *Mycena pura*[P], *Lepiota magnispora*[U], *Cystodermella lactea*[U], *Laccaria* sp.[U], *Cystoderma amianthinum*[E] and *Armillaria mellea*[E] | 1 | 20 | 0 | 0.00 | October 19, Yunnan |
| *Collybia* sp. | 1 | 7 | 0 | 0.00 | October 1, Guizhou |
| *Gymnopilus dilepis* | 10 | 34 | 0 | 0.00 | May 2 to June 9, Sichuan, Hunan, Chongqing; July 23, Fujian; October 28, Sichuan |
| ***Inocybe* aff. *decemgibbosa*** | 1 | 2 | 0 | 0.00 | May 21, Hunan |
| ***Inocybe* cf. *assimillata*** | 1 | 1 | 0 | 0.00 | November 27, Hunan |
| ***Inosperma* cf. *gregarium*** | 1 | 1 | 0 | 0.00 | September 22, Yunnan |
| *Inosperma hainanense* | 2 | 7 | 0 | 0.00 | August 9, Guangxi; September 30, Yunnan (5 Burmese) |
| *Inosperma muscarium* | 1 | 4 | 0 | 0.00 | May 20, Guangxi |
| *Laetiporus versisporus* | 1 | 1 | 0 | 0.00 | June 28, Yunnan |
| *Lanmaoa asiatica* | 12 | 14 | 0 | 0.00 | July 6 to October 20, Guangdong, Chongqing, Yunnan, Hunan (9 patients from 7 incidents ate boletes bought from Yunnan market) |
| *Panaeolus cyanescens* | 1 | 1 | 0 | 0.00 | September 12, Shandong |
| *Panaeolus subbalteatus* | 1 | 1 | 0 | 0.00 | July 1, Ningxia |
| *Pseudosperma citrinostipes* and ***Inocybe* aff. *pseudoreducta***[P] | 1 | 4 | 0 | 0.00 | July 3, Yunnan |
| *Pseudosperma umbrinellum* | 3 | 4 | 0 | 0.00 | August 31 to September 15, Ningxia |
| *Pseudosperma* sp. | 1 | 2 | 0 | 0.00 | May 17, Hunan |
| *Psilocybe cubensis* | 4 | 9 | 0 | 0.00 | March 29, Hunan; August 1 and 4, Hunan, Guangxi; November 2; Guangxi |
| *Psilocybe keralensis* | 1 | 1 | 0 | 0.00 | May 4, Fujian |
| *Psilocybe ovoideocystidiata* | 1 | 5 | 0 | 0.00 | May 1, Hubei |
| *Psilocybe samuiensis* | 2 | 2 | 0 | 0.00 | November 28 and December 3, Zhejiang, Hunan |
| **Photosensitive dermatitis** | | | | | |
| *Cordierites frondosus* | 1 | 3 | 0 | 0.00 | April 21, Chongqing |
| **Unclassified** | | | | | |
| *Amanita pseudoprinceps*[E] | 1 | 2 | 0 | 0.00 | August 12, Yunnan |

Continued

| Mushroom species | Number of incidents | Number of patients | Deaths | Case fatality (%) | Spatial and temporal distribution |
|---|---|---|---|---|---|
| *Armillaria gallica*$^{E}$ | 1 | 3 | 0 | 0.00 | May 6, Hunan (dried mushrooms, given by a friend from Northeast China) |
| *Armillaria mellea*$^{E}$ | 1 | 3 | 0 | 0.00 | November 10, Guizhou |
| *Boletus bainiugan*$^{E}$ and *B. reticuloceps*$^{E}$ | 1 | 28 | 0 | 0.00 | January 13, Yunnan (dried boletes, bought from market) |
| *Boletus bainiugan*$^{E}$ | 1 | 2 | 0 | 0.00 | August 8, Guangdong (bought from Yunnan market, eaten raw) |
| *Boletus bainiugan*$^{E}$, *Lanmaoa asiatica*$^{E,P}$, *Tricholomopsis rutilans*$^{G}$, *Caloboletus xiangtoushanensis*$^{U}$, *Imperator* sp.$^{U}$ and *Xerocomus* sp.$^{U}$ | 1 | 2 | 0 | 0.00 | July 16, Ningxia (dried boletes, given by a friend from Sichuan) |
| *Butyriboletus yicibus*$^{E}$ | 1 | 2 | 0 | 0.00 | July 29, Guangdong (bought from Yunnan market) |
| *Cortinarius sinensis*$^{E}$ | 1 | 2 | 0 | 0.00 | September 14, Ningxia |
| *Lanmaoa asiatica*$^{E,P}$, *Rubroboletus flammeus*$^{U}$, *Rubroboletus* sp.$^{U}$, *Clitocella orientalis*$^{U}$, *Imperator* sp.$^{U}$, *Caloboletus* sp.$^{U}$, *Inocybe* sp.$^{U}$, *Russula laurocerasi*$^{U}$ and *Russula mariae*$^{E}$ | 1 | 2 | 0 | 0.00 | August 5, Guizhou (dried boletes) |
| *Lepista nuda*$^{E,M}$ | 1 | 4 | 0 | 0.00 | September 12, Hebei |
| *Lycoperdon perlatum*$^{E,M}$ | 1 | 1 | 0 | 0.00 | May 27, Yunnan |
| *Macrocybe gigantea*$^{E,M}$ | 1 | 2 | 0 | 0.00 | May 25, Yunnan (was eaten raw) |
| *Pholiota spumosa*$^{E,M}$ | 1 | 3 | 0 | 0.00 | September 27, Sichuan |
| *Russula crustosa*$^{E}$ and *Laccaria yunnanensis*$^{E}$ | 1 | 6 | 0 | 0.00 | September 4, Sichuan |
| *Russula leucocarpa*$^{E}$ | 1 | 3 | 0 | 0.00 | August 6, Sichuan |
| *Russula leucocarpa*$^{E}$, *Russula densifolia*$^{E}$ and *Russula* sp.$^{U}$ | 1 | 2 | 0 | 0.00 | June 22, Sichuan |
| *Russula leucocarpa*$^{E}$ and *Amanita* sp.$^{U}$ | 1 | 2 | 0 | 0.00 | June 22, Sichuan |
| *Termitomyces fuliginosus*$^{E}$ | 1 | 1 | 0 | 0.00 | June 19, Sichuan |
| *Tricholoma terreum*$^{E}$ | 2 | 2 | 0 | 0.00 | March 1 and 5, Hunan |

Note: Species newly recorded as poisonous mushrooms in China are in italic bold.
Abbreviation: ALF=Acute liver failure; ARF=Acute renal failure; G=Gastroenteritis; P=Psycho to neurological disorder; M=Medicinal; U=Unclassified; E=Edible.

Preplanned Studies

# Survey of Residents' Satisfaction with the Environmental Sanitation of Key Public Places Under the Background of National Healthy City — China, 2021

Jiaxin Dong[1]; Qiqi Wang[1]; Jue Liu[2]; Hongyan Yao[1]; Xiao Qi[1]; Jianjun Liu[1,#]

**Summary**

**What is already known about this topic?**

Sanitation of public places has been the focus of environmental sanitation construction in China for many years. It is critical to achieving the goal of building national healthy cities and counties.

**What is added by this report?**

The results showed that in all types of areas, residents' satisfaction with the sanitation of railway stations and other places of transportation ranked first, and farmers' markets ranked last.

**What are the implications for public health practice?**

This study provides a suitable reference for government decision-makers to effectively improve the sanitation situation of key public places and to further construct national healthy cities and counties.

National healthy city establishment is an urban construction activity with Chinese characteristics. As an essential part of establishing national healthy cities, environmental sanitation covers many environmental hygiene-related issues. Among them, public place sanitation has been the focus and difficulty in China for many years, especially in key public places (small restaurants, small "internet cafes," small hairdressers, small dance halls, small hotels, and small bathrooms), which are ubiquitous. Public place sanitation has been a weak point in the efforts to achieve the goal of building national healthy cities (*1*). Residents are one of the stakeholders of the national healthy city construction policies and their subjective feelings can reflect the current situation to a certain extent. Moreover, the ultimate goal of the construction of national healthy cities is to improve health of residents, so knowing residents' ideas is essential. This study conducted a survey to evaluate residents' satisfaction with environmental sanitation in key places using a uniformly structured questionnaire to survey 32,243 residents of four provincial-level administrative divisions (PLADs). The results showed that in all types of areas, residents' satisfaction with the sanitation of railway stations and other places of transportation ranked first, and farmers' markets ranked last. It is recommended to strengthen research on the long-term management of the construction of national healthy cities and counties, formulate appropriate and effective policies, and provide more funds and personnel support for improving sanitation in key places.

In this study, the survey areas were determined by multistage sampling. Four PLADs that have a low ability to construct national healthy cities and counties — Hainan, Guizhou, Guangxi, and Sichuan — were selected for the survey area, with 10 districts, counties, and county-level cities chosen for each PLAD. Investigators did the survey from November 2021 to April 2022. The survey tool was the "Questionnaire on Residents' Satisfaction with Environmental Sanitation," which mainly included the basic information of the respondents, general information of the survey area, satisfaction with environmental sanitation (city-appearance and environmental sanitation, environmental sanitation management, water sanitation, and sanitation of key public places), and the problems that the respondents think exist in environmental sanitation. The questionnaire items were scored with Likert's 5-level scoring method, with 1=very dissatisfied, 2=dissatisfied, 3=average, 4=satisfied, and 5=very satisfied. The overall satisfaction of residents with the sanitation of key public places is divided into two categories. "Satisfied, very satisfied" was classified as "satisfied", and "very dissatisfied, dissatisfied, general" was classified as "dissatisfied". Residents are selected by quota sampling. Based on the 2019 population data of each district and county sampled, the gender distribution and age distribution of the sampled population were consistent with the total population. The inclusion criteria of the residents were: living in the survey area for 6 months or more, age ≥18 years, having clear cognitive and understanding ability, and being willing to participate in the questionnaire. The sample size of this study was calculated with the formula N=$\frac{\mu_{\alpha/2}^{2} \times \pi \times (1-\pi)}{\delta^{2}} \times deff$ and the sample size of each PLAD was 4,609. Considering the non-response rate of 10%, the sample size required by each PLAD is about 5,000.

Uniformly trained investigators conducted surveys in the form of central intercept investigations. The investigator introduced the purpose of the investigation to the respondents and obtained the informed consent of them, and the respondents filled in the survey themselves. Among them, elderly and less educated residents filled out questionnaires under the guidance of the investigator. Data were cleaned in Microsoft Office Excel (version 2016; Microsoft Corp., Washington, USA), and analyzed with SPSS Statistics (version 22.0, IBM Corporation, Armonk, USA). Counts were expressed as *n* (%) and chi-squared tests were used for comparisons. Statistical tests were two-tailed and $P$<0.05 was considered significant.

A total of 32,243 residents participated in the survey, with a response rate of 100% and an average age of 39.19±11.87 years. Among them, 11,573 (35.9%) were male, 19,646 (60.9%) had junior college and bachelor degrees, 19,024 (59.0%) resided in urban areas, and 18,209 (56.5%) had lived in the survey area for more than 10 years. The results of $\chi^2$ test show that the overall satisfaction of residents with the sanitation of key public places had statistical significance in terms of gender ($\chi^2$=437,659, $P$<0.001), education degree ($\chi^2$=121.071, $P$<0.001), age ($\chi^2$=519.803, $P$<0.001), occupation ($\chi^2$=556.669, $P$<0.001), living area ($\chi^2$=312.909, $P$<0.001), living time ($\chi^2$=11.292, $P$<0.001), etc. (Table 1).

The survey areas selected in this study are 11 cities and 29 counties, including 9 national healthy cities and 16 national healthy counties. The overall satisfaction of residents with the environmental sanitation status of key public places in national healthy cities was 62.9% [95% confidence interval (*CI*): 61.6%–64.2%], which was higher than that of non-national healthy cities (47.4%, 95% *CI*: 45.4%–49.3%). Among them, in national healthy cities, residents' satisfaction with the sanitary conditions of recreation places (59.2%, 95% *CI*: 57.8%–60.5%) and farmers markets (57.1%, 95% *CI*: 55.7%–58.4%) was lower, but higher than that of non-national healthy city residents with the sanitary conditions of recreation places (45.9%, 95% *CI*: 43.9%–47.9%) and farmers markets (36.8%, 95% *CI*: 34.9%–38.7%) (Table 2).

The overall satisfaction of residents with the environmental sanitation status of key public places in national healthy counties was 44.8% (95% *CI*: 44.0%–45.7%), which was lower than that of non-national healthy counties (62.3%, 95% *CI*: 61.4%–63.2%). Among them, in national healthy counties, residents' satisfaction with the sanitary conditions of beauty salon places (41.2%, 95% *CI*: 40.2%–42.1%) and farmers markets (38.6%, 95% *CI*: 37.8%–39.4%) was lower. And in non-national healthy counties, residents' satisfaction with the sanitary conditions of recreation places (59.8%, 95% *CI*: 58.9%–60.7%) and farmers markets (56.0%, 95% *CI*: 55.0%–56.9%) was lower (Table 3).

## DISCUSSION

The results showed that among the four types of areas, the health satisfaction of farmers' markets was the lowest. It is speculated that the reasons for the above situation may be: the infrastructure of some farmers' markets is backward, the capital investment is insufficient, environmental health regulation is difficult, some citizens have poor awareness of environmental sanitation, which makes cleaning work hard, and the market is a public place with concentrated human flows and complex logistics. Due to the lack of cold chain logistics and storage facilities, rats breed easily and are difficult to control (*2–3*).

It is noteworthy that residents in national healthy cities are more satisfied with various public places than those in non-national healthy cities, while the opposite is true in national healthy counties. The reasons may be that some national healthy counties have experienced a decline in work and rebounding problems, so residents give an "unsatisfactory" evaluation compared with the health status during the establishment of national healthy cities and towns (*4*), which also indicates that exploring the establishment of a long-term management mechanism for national healthy cities and towns is necessary. In addition, the satisfaction rate reflects the gap between individual expectations and actual feelings. The smaller the gap, the higher the satisfaction rate. Low satisfaction does not mean an absolute decline of the work. It is likely that the improvement speed of the work level lags

TABLE 1. Basic information of residents' health satisfaction in key public places surveyed in four provincial-level administrative divisions ($n$=32,243, %).

| Variable | Total | Satisfied | | $\chi^2$ | $P$ |
|---|---|---|---|---|---|
| | | $n$ | rate (95% $CI$) | | |
| Gender | | | | 437.659 | <0.001 |
| Female | 20,670 | 10,210 | 49.4 (48.7–50.1) | | |
| Male | 11,573 | 7,118 | 61.5 (60.6–62.4) | | |
| Level of education | | | | 121.071 | <0.001 |
| Junior high school and below | 6,049 | 2,923 | 48.3 (47.1–49.6) | | |
| Technical secondary school/senior high school/technical school | 6,221 | 3,226 | 51.9 (50.6–53.1) | | |
| Junior college/bachelor degrees | 19,646 | 10,988 | 55.9 (55.2–56.6) | | |
| Postgraduate and above | 327 | 191 | 58.4 (53.0–63.8) | | |
| Age (years) | | | | 519.803 | <0.001 |
| 18–44 | 22,360 | 11,165 | 49.9 (49.3–50.6) | | |
| 45–59 | 7,475 | 4,455 | 59.6 (58.5–60.7) | | |
| ≥60 | 2,408 | 1,708 | 70.9 (69.1–72.7) | | |
| Occupation | | | | 556.669 | <0.001 |
| Students | 452 | 219 | 48.5 (43.8–53.1) | | |
| TAP* | 12,934 | 6,858 | 53.0 (52.2–53.9) | | |
| Business and service personnel | 2,361 | 1,210 | 51.2 (49.2–53.3) | | |
| Managers of government agencies, enterprises and institutions | 5,977 | 3,822 | 63.9 (62.7–65.2) | | |
| Retired | 1,238 | 859 | 69.4 (66.8–72.0) | | |
| Unemployed and others | 9,281 | 4,360 | 47.0 (46.0–48.0) | | |
| Living area | | | | 312.909 | <0.001 |
| Suburban (rural) and other | 13,219 | 6,335 | 47.9 (47.1–48.8) | | |
| Other densely populated urban areas (residential areas) | 9,049 | 5,133 | 56.7 (55.7–57.7) | | |
| Central urban area (where businesses gather or traffic is heavy) | 9,975 | 5,860 | 58.7 (57.8–59.7) | | |
| Living time | | | | 11.292 | <0.001 |
| 6 months to 3 years | 4,482 | 2,314 | 51.6 (50.2–53.1) | | |
| 3 to 10 years | 9,552 | 5,221 | 54.7 (53.7–55.7) | | |
| >10 years | 18,209 | 9,793 | 53.8 (53.1–54.5) | | |
| Areas type | | | | 79.684 | <0.001 |
| City (District) | 7,715 | 4,466 | 57.9 (56.8–59.0) | | |
| County | 24,528 | 12,773 | 52.1 (51.4–52.7) | | |

* T refers to professional technicians; A refers to agriculture, forestry, animal husbandry, fishery and water conservancy production personnel; P refers to production and transportation equipment operators.

behind the improvement speed of the masses' expectations (*5*), it is also possible that different residents have different standards for evaluating satisfaction.

Previous studies on sanitation of public places mainly focused on evaluating whether the sanitation of each was qualified by sampling and monitoring the public goods or air quality of each place (*6–7*). These studies focused on discussing the current problems and corresponding remediation plans from the perspective of health supervision and management (*8*), but rarely evaluated the sanitation of the public place and collected ideas from the perspective of residents. This study investigated the environmental sanitation conditions of key public places by knowing the satisfaction of residents. Lessons learned will inform the subsequent construction of national healthy cities and counties.

This study has some limitations. Firstly, central intercept investigation was adopted to select residents.

TABLE 2. Comparative analysis of residents' satisfaction with the environmental sanitation of key public places in different types of cities ($n$=7,715, %).

| City type | Total | | Farmers market | | Beauty salon places | | Recreation places | | Accommodation places | | Food and beverage places | | Railway stations and other transportation places | |
|---|---|---|---|---|---|---|---|---|---|---|---|---|---|---|
| | $n$ | Rate (95% $CI$) | $n$ | Rate (95% $CI$) | $n$ | Rate (95% $CI$) | $n$ | Rate (95% $CI$) | $n$ | Rate (95% $CI$) | $n$ | Rate (95% $CI$) | $n$ | Rate (95% $CI$) |
| Non-national healthy cities | 1,175 | 47.4 (45.4–49.3) | 913 | 36.8 (34.9–38.7) | 1,190 | 48.0 (46.0–49.9) | 1,139 | 45.9 (43.9–47.9) | 1,174 | 47.3 (45.4–49.3) | 1,171 | 47.2 (45.2–49.2) | 1,252 | 50.5 (48.5–52.4) |
| National healthy cities | 3,291 | 62.9 (61.6–64.2) | 2,986 | 57.1 (55.7–58.4) | 3,268 | 62.4 (61.1–63.8) | 3,097 | 59.2 (57.8–60.5) | 3,211 | 61.3 (60.0–62.7) | 3,184 | 60.8 (59.5–62.2) | 3,523 | 67.3 (66.0–68.6) |
| $\chi^2$ | 166.252 | | 276.122 | | 144.537 | | 119.563 | | 135.036 | | 127.273 | | 202.530 | |
| $P$ | 0.001 | | 0.001 | | 0.001 | | 0.001 | | 0.001 | | 0.001 | | 0.001 | |

Abbreviation: $CI$=confidence interval.

TABLE 3. Comparative analysis of residents' satisfaction with the environmental sanitation of key public places in different types of counties ($n$=24,528, %).

| County type | Total | | Farmers market | | Beauty salon places | | Recreation places | | Accommodation places | | Food and beverage places | | Railway stations and other transportation places | |
|---|---|---|---|---|---|---|---|---|---|---|---|---|---|---|
| | $n$ | Rate (95% $CI$) | $n$ | Rate (95% $CI$) | $n$ | Rate (95% $CI$) | $n$ | Rate (95% $CI$) | $n$ | Rate (95% $CI$) | $n$ | Rate (95% $CI$) | $n$ | Rate (95% $CI$) |
| Non-national healthy counties | 6,651 | 62.3 (61.4−63.2) | 5,976 | 56.0 (55.0−56.9) | 6,583 | 61.7 (60.8−62.6) | 6,382 | 59.8 (58.9−60.7) | 6,580 | 61.6 (60.7−62.6) | 6,547 | 61.3 (60.4−62.3) | 7,085 | 66.4 (65.5−67.3) |
| National healthy counties | 6,211 | 44.8 (44.0−45.7) | 5,346 | 38.6 (37.8−39.4) | 4,459 | 41.2 (40.2−42.1) | 5,776 | 41.7 (40.9−42.5) | 6,125 | 44.2 (43.4−45.0) | 6,052 | 43.7 (42.9−44.5) | 7,029 | 50.7 (49.9−51.6) |
| $\chi^2$ | 738.484 | | 734.324 | | 673.103 | | 789.958 | | 733.938 | | 751.975 | | 603.629 | |
| $P$ | 0.001 | | 0.001 | | 0.001 | | 0.001 | | 0.001 | | 0.001 | | 0.001 | |

Abbreviation: $CI$=confidence interval.

Although the study had broad geographic coverage and a large sample size in four PLADs, the representation of the participants may have been limited. Secondly, this survey only described the residents' satisfaction with the sanitation of key public places, and failed to consider the residents' awareness of environmental sanitation and other factors that may affect residents' satisfaction. This study provides a suitable reference for government decision-makers to effectively improve the sanitation situation of key public places and further construct national healthy cities and counties.

**Conflicts of interest**: No conflicts of interest.

**Funding:** Performance and operation project of the Chinese Preventive Medicine Association (2022); Operation of public health emergency response mechanism of China CDC (131031001000210001).

**doi:** 10.46234/ccdcw2023.010

# Corresponding author: Jianjun Liu, liujj@chinacdc.cn.

[1] Chinese Center for Disease Control and Prevention, Beijing, China; [2] School of Public Health, Peking University, Beijing, China.

Submitted: November 17, 2022; Accepted: January 17, 2023

## REFERENCES

1. Che QZ, Wang Y, Gao SM. Discussion on the establishment of national healthy city and the regulation of "six small" industries. Pract Prev Med 2005;12(3):712 – 3. http://dx.doi.org/10.3969/j.issn.1006-3110.2005.03.139. (In Chinese).
2. Chen JL. Managing the farmer's market to make citizens' life better --education research report on the theme of "Don't forget your original intention and keep your mission in mind". China Market Regul Res 2019(10):14 – 8. https://kns.cnki.net/kcms2/article/abstract?v=2pc-UOsZbJnrKorR-qD5Ysj_CD8JJfsgRtrDKtHW5yFYlTg5nJhdj7tLpdICGpV0Nu8kuMWBNr6iq6a3CIOehl2sBqZQoIo2VZvJhZwFuuinBUwsSiG0JV95aqmyPcme&uniplatform=NZKPT. (In Chinese).
3. Qian C, Li Y, Li P, Chen M. Thinking on the planning and construction of Chongqing agricultural trade market in response to major public health events. In: Proceedings of the 2020 China urban planning annual conference. Chengdu. 2021;p.1-8. https://kns.cnki.net/kcms2/article/abstract?v=3uoqIhG8C467SBiOvrai6TdxYiSzCnOEEIKB-6S51JyFOld47yB1sKgi83M_Pv5h5PDN5ioY3WD0_rXr1PpJI7Z7_-PRtMt98HxRRU_fxMA%3d&uniplatform=NZKPT. (In Chinese).
4. Zhang Y, Feng L, Zheng CL, Fu XJ, Tian ZY, Huang GF, et al. Analysis on the awareness rate and satisfaction of urban residents in Yunnan on the "7 special campaigns" for patriotic health in 2020. J Med Pest Control 2022;38(5):489 – 92. http://dx.doi.org/10.7629/yxdwfz202205020. (In Chinese).
5. Mao TJ, Hu W, Yang F. Analysis on the role of mass satisfaction survey in long-term management of national healthy cities. Zhejiang Prev Med 2015;27(5):529 – 31. http://dx.doi.org/10.19485/j.cnki.issn1007-0931.2015.05.033. (In Chinese).
6. Wan BY, Zhang MY, Li WJ. Analysis on sanitary conditions of 104 public places in Chaoyang District of Beijing in 2019. Chronic Pathematol J 2021;22(8):1191 – 3. http://dx.doi.org/10.16440/J.CNKI.1674-8166.2021.08.11. (In Chinese).
7. Fu BB, Zhang L, Xu Y, Tan XD. Analysis of healthy monitoring results of public places in Hongshan district of Wuhan from 2018 to 2020. Health Educ Health Promot 2022;17(2):177 – 81. http://dx.doi.org/10.16117/j.cnki.31-1974/r.202202177. (In Chinese).
8. Bai JH. Problems of sanitation supervision in public places and the countermeasures. Chin Rural Health Serv Adm 2020;40(2):137 – 40. http://dx.doi.org/10.3969/j.issn.1005-5916.2020.02.016. (In Chinese).

Preplanned Studies

# Transmission Dynamics and Epidemiological Characteristics of the SARS-CoV-2 Delta Variant — Hunan Province, China, 2021

Kaiwei Luo[1,&]; Yanpeng Wu[2,&]; Yan Wang[3]; Ziyan Liu[1]; Lan Yi[2]; Shanlu Zhao[1]; Xuemei Yan[3]; Hao Yang[1]; Kaiyuan Sun[4]; Marco Ajelli[5]; Shixiong Hu[1,#]; Hongjie Yu[2,3,#]

**Summary**

**What is already known about this topic?**

Little is known about the epidemiology, natural history, and transmission patterns of the severe acute respiratory syndrome coronavirus 2 (SARS-CoV-2) Delta variant. Monitoring the evolution of viral fitness of SARS-CoV-2 in the host population is key for preparedness and response planning.

**What is added by this report?**

We analyzed a successfully contained local outbreak of Delta that took place in Hunan, China, and provided estimates of time-to-key event periods, infectiousness over time, and risk factors for SARS-CoV-2 infection and transmission for a still poorly understood variant.

**What are the implications for public health practice?**

Our findings simultaneously shed light on both the characteristics of the Delta variant, by identifying key age groups, risk factors, and transmission pathways, and planning a future response effort against SARS-CoV-2.

Monitoring changes in the epidemiologic features between different severe acute respiratory syndrome coronavirus 2 (SARS-CoV-2) variants is key to understanding the evolution of viral fitness in the host population. Here, we analyzed a successfully contained local outbreak of the Delta variant that took place in Hunan, China, in July–August, 2021. Detailed data on SARS-CoV-2 infections and their contacts were collected during the outbreak. By leveraging these data, we estimated key epidemiological parameters, including the incubation period, serial interval, and generation time. We constructed a generalized linear mixed-effects model (GLMM) to quantify risk factors for Delta infection and transmission. Between July 28 and August 15, 2021, a total of 129 infections and their 2,118 close contacts were identified during the outbreak in Hunan Province. The mean incubation period, serial interval, and generation time were estimated to be 5.3 days [interquartile range (IQR): 3.0–6.5], 4.3 days (IQR: 1.7–6.8), and 4.4 days (IQR: 2.4–5.8), respectively. Infectiousness peaked 1.6 days before symptom onset, with 63.0% of the transmission events occurring during the presymptomatic phase. Household contacts had the highest risk of infection [odds ratio (*OR*)=6.79, 95% confidence interval (*CI*): 3.20–14.44]. The susceptibility to Delta infection was higher in children aged 0–9 years than in adults aged 18–64 years (*OR*=2.44, 95% *CI*: 1.03–5.80). The effectiveness of the inactivated vaccine against any confirmed infection was 54% (95% *CI*: 7%–77%). By providing quantitative evidence about key epidemiological features as well as infection and transmission risk factors for Delta, our findings improved our relatively scarce understanding of this variant of concern and, more broadly, the evolutionary trajectory of SARS-CoV-2.

During the 2021 Delta outbreak in Hunan, field epidemiological investigations allowed the prompt identification of the population at risk, including contacts of positive individuals. Here we provided descriptive statistics of positive cases' characteristics and close contacts. We estimated the incubation period (i.e., the time delay from infection to illness onset), serial interval (i.e., the time interval between the onset of symptoms in a primary infector and their onset in secondary infections), generation time (i.e., the time interval between infection of the primary infector and their secondary infections), and infectiousness profile (i.e., the temporal distribution of the probability of transmission), following the method in reference (*1*). To evaluate the impact of nonpharmaceutical interventions (NPIs) on the containment of the outbreak, we also compared the distribution of the time delay from symptom onset to hospitalization, to isolation, to the collection of the first positive specimen, and laboratory confirmation before and after the implementation of NPIs using the Kolmogorov-

Smirnov test (K-S test).

A GLMM was used to quantify the effects of potential drivers of susceptibility to Delta variant infection and infectivity of infected individuals. To quantify the vaccination effectiveness against the Delta variant infection and transmission, we incorporated the vaccination status of infectors and contacts into the model. Other factors, including age, sex, and the contact setting, could be potential drivers of the susceptibility and infectivity of SARS-CoV-2 ancestral strains in a previous research (*1*) and thus have also been considered in our models. (Supplementary Material, available in https://weekly.chinacdc.cn/). All vaccinated individuals included in this study received inactivated vaccines. Our primary analysis was based on 2,004 close contacts, and a supplementary analysis was conducted incorporating another 4,131 general contacts aged under 65 years. Statistical analyses were performed in R, version 4.1.1 (R Foundation for Statistical Computing, Vienna, Austria).

The first local infection of Delta in Hunan Province, China, was identified on July 28, 2021: an individual who shared the same boat with domestically infected tourists (*2*). Between July 28 and August 15, 2021, 129 SARS-CoV-2 Delta infections were identified in Hunan Province, China. According to genomic data, all identified infections in this outbreak were infected by the Delta variant.

The outbreak quickly spread from the original touristic location through other cities within Hunan Province (Supplementary Figure S1, available in https://weekly.chinacdc.cn/). Through epidemiological investigations and active contact tracing, 10,971 individuals categorized as the at-risk population were initially identified, of which 2,118 were further classified as close contacts of infected individuals. Another 4,513 were identified as general contacts (Supplementary Figure S2, available in https://weekly.chinacdc.cn/), and the reconstructed transmission chain was reported in Supplementary Figure S3 (available in https://weekly.chinacdc.cn/). Among all infections, 19 were asymptomatic, and 110 were symptomatic, including 48 mild cases (43.6%), 61 moderate cases (55.5%), and 1 severe case (0.9%), with no critical cases or deaths reported [Table 1, see Supplementary Table S1 (available in https://weekly.chinacdc.cn/) for an analysis of the completeness of the variables].

We analyzed 71 locally confirmed cases with clear exposure dates or exposure windows to estimate the incubation period. From the best-fitting lognormal distribution, we obtained a mean estimate of the incubation period of 5.3 days (median: 4.4, IQR: 3.0–6.5). Consistent results were obtained when fitting alternative distributions (Supplementary Table S2, available in https://weekly.chinacdc.cn/). The symptom onset date was available for 54 transmission pairs; the resulting serial interval had an estimated mean of 4.3 days (median: 4.2, IQR: 1.7–6.8), based on fitting a Weibull distribution, and consistent results were found by fitting alternative distributions (Supplementary Table S2). Infectiousness was estimated to peak 1.6 days before symptom onset, and the proportion of pre-symptomatic transmission was 63.0%, with 95% of transmission events occurring between −5.6 and 5.8 days after the date of symptom onset. The mean generation time was estimated to be 4.4 days (median: 3.9, IQR: 2.4–5.8) (Figure 1A–B). A marked decreasing trend was observed in all time intervals from symptom onset to hospitalization, to isolation, to the collection of the first positive specimen, and the laboratory diagnosis of symptomatic individuals after the initiation of NPIs. Among them, the time interval from symptom onset to isolation showed the most significant decrease, with a reduction from a median of 4.0 days (IQR: 2.5–7.0) to 0 days (IQR: −1.0–1.0) (Figure 1C), which may have potentially played a crucial role in the successful containment of the outbreak.

A multivariate regression analysis was performed based on close contact data collected. The results showed that the susceptibility to infection of the adult population was lower for fully vaccinated individuals than non-vaccinated individuals (*OR*=0.46, 95% *CI*: 0.23–0.93), indicating a vaccine effectiveness of 54% (95% *CI*: 7%–77%) against any confirmed Delta infection. Among unvaccinated close contacts, susceptibility to Delta infection was higher in children than in adults (*OR*=2.44, 95% *CI*: 1.03–5.80). In addition, we found a higher infection risk in the household setting (*OR*=6.79, 95% *CI*: 3.20–14.44), while other potential risk factors, such as the sex of the infectors and the contacts, were not statistically significant (Table 2). In Supplementary Table S3 (available in https://weekly.chinacdc.cn/), we present the results of a sensitivity analysis where, when the source of exposure was not resolved, the potential infector was selected at random. The consistency between these results and those of the main analysis supports the robustness of our main conclusions. A supplementary analysis was performed on 6,135

TABLE 1. Characteristics of SARS-CoV-2 Delta infected individuals and their close contacts in Hunan Province, China, 2021.

| Characteristics | Infections (*n*=129) | Close contacts (*n*=2,118) | Secondary infection attack rate (%, 95% *CI*)* |
|---|---|---|---|
| Age, years | | | |
| Median (IQR) | 34 (15, 48) | 34 (20, 46) | |
| Age group, years | | | |
| 0–9 | 19 (14.7%) | 140 (6.6%) | 10.7 (6.1, 17.1) |
| 10–17 | 19 (14.7%) | 293 (13.8%) | 4.8 (2.6, 7.9) |
| 18–64 | 87 (67.4%) | 1,595 (75.3%) | 3.2 (2.4, 4.2) |
| >65 | 4 (3.1%) | 90 (4.2%) | 4.4 (1.2, 11) |
| Sex | | | |
| Male | 58 (45.0%) | 920 (43.4%) | 4.6 (3.3, 6.1) |
| Female | 71 (55.0%) | 1,198 (56.6%) | 3.5 (2.5, 4.7) |
| Clinical outcome | | | |
| Not infected | – | 2,034 (96.0%) | |
| Confirmed asymptomatic infection | 19 (14.7%) | 9 (0.4%) | |
| Confirmed symptomatic infection | 110 (85.3%) | 75 (3.5%) | |
| Mild | 48 (43.6%) | 39 (52.0%) | |
| Moderate | 61 (55.5%) | 35 (46.7%) | |
| Severe | 1 (0.9%) | 1 (1.3%) | |
| Vaccination history† | | | |
| Unvaccinated | 66 (51.2%) | 993 (46.9%) | 5.2 (3.9, 6.8) |
| Partially vaccinated | 27 (20.9%) | 290 (13.7%) | 4.8 (2.7, 8.0) |
| Time interval between last vaccination and symptoms onset or last exposure, days§ | | | |
| Median (IQR) | 26 (21, 35) | 25 (21, 28) | |
| Fully vaccinated | 36 (27.9%) | 835 (39.4%) | 2.2 (1.3, 3.4) |
| Time interval between last vaccination and symptoms onset or last exposure, days§ | | | |
| Median (IQR) | 49 (40, 54) | 48 (41, 56) | |
| Mode of detection | | | |
| Passive surveillance | 14 (10.9%) | – | |
| Contact tracing | 80 (62.0%) | – | |
| Community screening | 35 (27.1%) | – | |

Note: "−" means data not available.The last column provided the secondary infection attack rates across different groups of age, sex, and vaccination history.

Abbreviation: IQR=interquartile range; *CI*=confidence interval; SARS-CoV-2=severe acute respiratory syndrome coronavirus 2; COVID-19=coronavirus disease 2019.

* The secondary infection attack rate was calculated by dividing the number of infections by the total number of close contacts.

† Vaccination history: 1) unvaccinated (i.e., individuals who did not receive any COVID-19 vaccines or received 1 dose of COVID-19 vaccine less than 14 days before the date of the last known contact); 2) partially vaccinated (i.e., individuals who had received either 1 dose of a COVID-19 vaccine or received 2 doses of vaccines with the date of the second dose less than 14 days before the date of the last known contact) and 3) fully vaccinated (i.e., individuals who completed the full 2-dose course vaccination more than 14 days before the date of the last known contact).

§ For the asymptomatic subjects and the cases diagnosed by imaging characteristics, we used the date of the first sample collection with a positive test instead of the date of symptom onset.

contacts, which included both close contacts and general contacts, and these results are also consistent with those of the main analysis (Supplementary Table S4, available in https://weekly.chinacdc.cn/).

## DISCUSSION

Based on case surveillance and contact tracing data, we described the epidemiological characteristics of the

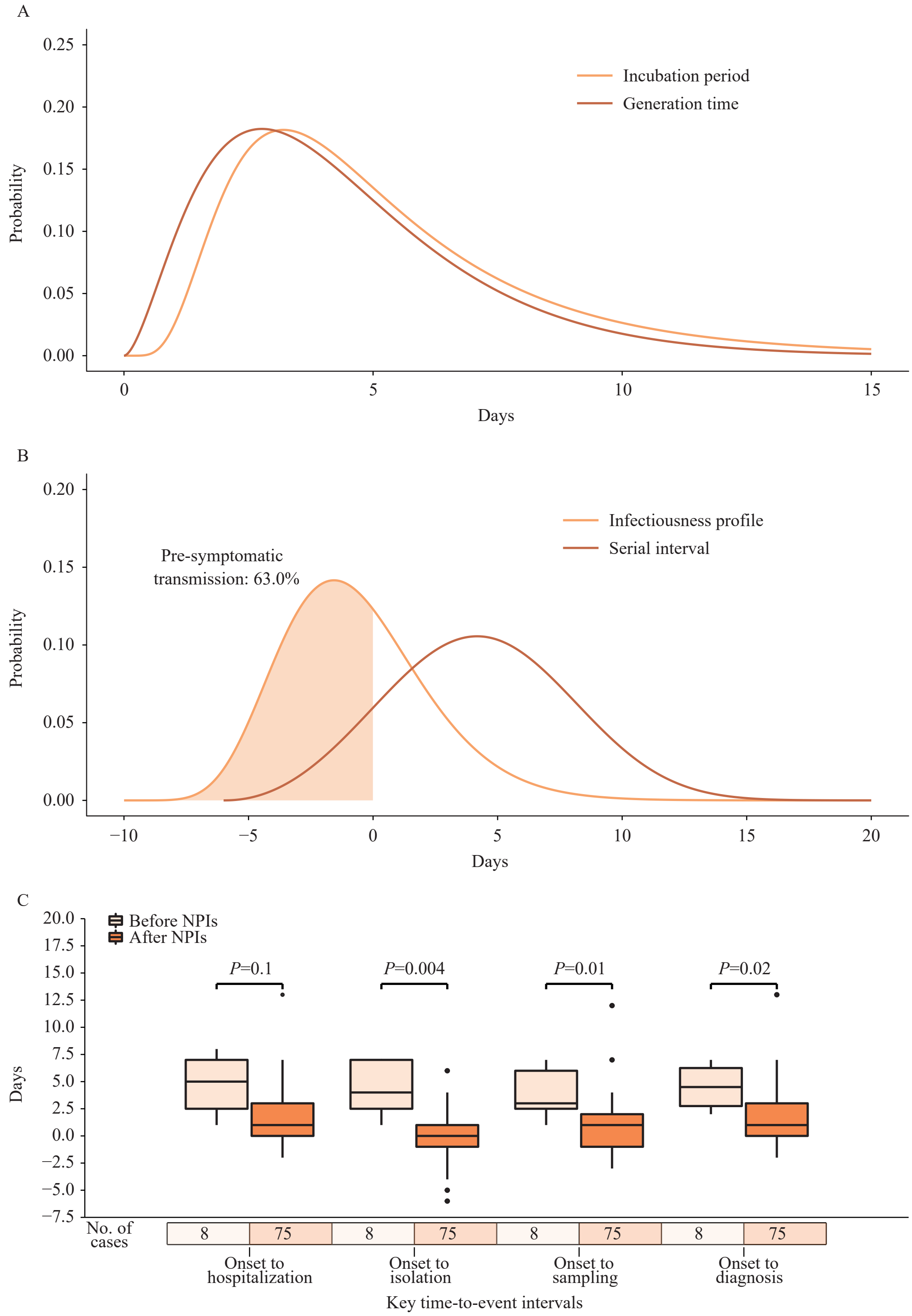


FIGURE 1. Key time-to-event intervals of SARS-CoV-2 Delta infections in Hunan, China. (A) Estimated incubation period distribution by log-normal distributions and generation time by gamma distributions based on 71 confirmed cases. (B) Estimated distribution of the serial interval by Weibull distributions and of the infectiousness profile by gamma distributions based on 54 transmission pairs. (C) Time intervals from symptom onset to hospitalization, isolation, first time of sampling, and diagnosis of symptomatic cases before and after the implementation of NPIs.
Note: The infectiousness profile describes the infectiousness of an individual over time since the onset of symptoms.
Abbreviation: NPIs=nonpharmaceutical interventions; SARS-CoV-2=severe acute respiratory syndrome coronavirus 2.

TABLE 2. Estimating the association of potential risk factors with the risk of acquiring and transmitting the SARS-CoV-2 Delta variant.

| Characteristic | Univariate analysis | | Multivariate analysis | |
|---|---|---|---|---|
| | ***OR* (95% *CI*)** | ***P* value** | ***OR* (95% *CI*)** | ***P* value** |
| Age (years) and vaccination status of contacts† | | | | |
| Unvaccinated children (0–9 years) | 3.42 (1.49, 7.89) | 0.004** | 2.44 (1.03, 5.80) | 0.044* |
| Unvaccinated adolescents (10–17 years) | 1.56 (0.66, 3.69) | 0.310 | 1.20 (0.46, 3.10) | 0.707 |
| Unvaccinated adults (18–64 years) | Reference | | Reference | |
| Vaccinated adults (18–64 years) | 0.49 (0.25, 0.95) | 0.035* | 0.46 (0.23, 0.93) | 0.030* |
| Age (years) and vaccination status of infectors§ | | | | |
| Unvaccinated children (0–9 years) | 1.79 (0.45, 7.19) | 0.410 | 0.82 (0.19, 3.46) | 0.784 |
| Unvaccinated adolescents (10–17 years) | 0.32 (0.07, 1.51) | 0.149 | 0.63 (0.16, 2.52) | 0.513 |
| Unvaccinated adults (18–64 years) | Reference | | Reference | |
| Vaccinated adults (18–64 years) | 0.53 (0.17, 1.61) | 0.260 | 0.51 (0.19, 1.40) | 0.192 |
| Type of contact | | | | |
| Household contact | 7.54 (3.67, 15.48) | <0.001*** | 6.79 (3.20, 14.44) | <0.001*** |
| Health care | 0.44 (0.10, 1.93) | 0.274 | 0.22 (0.04, 1.11) | 0.067 |
| Social contact | Reference | | Reference | |
| Workplace contact | 0.64 (0.15, 2.75) | 0.550 | 0.73 (0.17, 3.20) | 0.678 |
| Other | 0.07 (0.02, 0.20) | <0.001*** | 0.05 (0.02, 0.15) | <0.001*** |
| Sex of contacts | | | | |
| Female | Reference | | Reference | |
| Male | 1.03 (0.62, 1.73) | 0.906 | 0.72 (0.40, 1.28) | 0.261 |
| Sex of infectors | | | | |
| Female | Reference | | Reference | |
| Male | 1.04 (0.39, 2.79) | 0.942 | 0.67 (0.27, 1.67) | 0.391 |
| Clinical severity of primary cases | | | | |
| Asymptomatic infection | Reference | | − | − |
| Symptomatic infection | 1.05 (0.23, 4.75) | 0.951 | − | − |

Note: "−" in the column of "*OR* (95% *CI*)" indicated that the corresponding variable was not incorporated into the analysis. All children and adolescents (under 18 years) were unvaccinated, as they were not covered by the COVID-19 vaccination program in the Chinese mainland during the Delta outbreak. Vaccinated adults denote fully vaccinated adults, while partially vaccinated adults were deemed unvaccinated adults in the analysis.

Abbreviation: *CI*=confidence interval; *OR*=odds ratio; COVID-19=coronavirus disease 2019; SARS-CoV-2=severe acute respiratory syndrome coronavirus 2.

* *P*<0.05,

** *P*<0.01.

*** *P*<0.001.

† Contacts who were aged at or over 65 years or whose infectors were aged at or over 65 years were excluded from this analysis due to the small sample size.

§ For a contact who had interacted with more than one SARS-CoV-2 infection, we chose the first infected individual they had been exposed to as the potential infector. If they had exposed to multiple infectors at the same time, we randomly chose one from among these infectors as the potential infector.

SARS-CoV-2 Delta variant outbreak in Hunan Province, China, in July–August 2021. To date, only a few studies have provided estimates of the incubation period, serial interval, and generation time of Delta variant infection. These studies suggest that the mean (or median) incubation period of Delta ranges from 3.0 to 6.0 days (*3*–*4*), which contains the mean estimate obtained in our study (5.3 days); also, our estimate of the serial interval (4.3 days) falls inside the range reported in previous studies (range 2.6–5.4 days) (*5*–*6*). Regarding the generation time, we found only two studies providing estimates for the Delta variant; the first one was conducted in the UK and found a mean value of 4.7 days (*7*), while the second one was conducted in Italy and found a mean value of 6.6 days (*6*). By comparison, we estimated a mean generation time of 4.4 days. However, it is important to stress that here we provide estimates of the "realized" (i.e., observed) generation time. In contrast the two European studies estimate the intrinsic generation time (i.e., what would be observed in an infinitely large and fully susceptible population). Contact tracing could speed up the detection and isolation of infectors, and case isolation and contact quarantine could prevent potential infectors from contacting susceptible individuals, which limited our estimates to the specific conditions of the analyzed outbreak. A strength of our study is that our estimates of the time-to-event distributions are based on transmission pairs of the entire outbreak and are thus insensitive to right-censoring bias mediated by epidemic growth rates (*8*).

Different from the ancestral strain, we found that children were more likely to be infected with the Delta variant, and similar observations have been found in other settings (*9*). This finding emphasizes the relevance of young individuals in SARS-CoV-2 outbreaks. In agreement with prior studies (*10*), the effectiveness of 2 doses of inactivated vaccines against Delta infection was estimated at 54% (*OR*=0.46, 95% *CI*: 0.23–0.93), while their effectiveness in preventing forward transmission was not statistically significant, possibly due to the small sample size. Our analysis did not explicitly consider the effect of the waning of vaccine protection as most [86% (31/36)] reported infections among fully vaccinated individuals were infected within two months after receiving their most recent vaccine dose. Nonetheless, our study further supports the key role of vaccination in mitigating coronavirus disease 2019 (COVID-19) burden.

Our study has several limitations. First, the sample size of our study is relatively limited (129 confirmed infections, 2,118 contacts, and 4,513 general contacts). It thus does not allow the analysis for further stratifications, such as the estimation of the key time-to-event intervals by vaccination status. Moreover, it is possible that our sample size is insufficient to provide statistically significant results for reducing forward transmission in vaccinated individuals. Second, due to the small number of asymptomatic infections in our sample, we did not distinguish between asymptomatic and symptomatic infections in our analysis, which may mask the heterogeneity of the two modes of transmission. The low proportion of asymptomatic infections in our sample (14.7%) as compared to more recent studies on outbreaks of the Omicron variants (*11*) may be due to several factors, including the reliance on repeated city-wide screenings of the population to curb the spread of highly transmissible Omicron variants (*12*), the progressive increase of population immunity protecting against symptomatic disease, and a possible reduced intrinsic severity of the Omicron variants (*13*).

Given the rapid adaptive evolution of SARS-CoV-2, having a cohesive picture of the differences and similarities between different variants is key for preparedness planning. As such, our findings not only shed light on the characteristics of the analyzed outbreak but can also be instrumental for planning future response efforts against SARS-CoV-2.

**Acknowledgments**: All the teams of field investigators of the Hunan Provincial Center for Disease Control and Prevention for their contribution.

**Funding:** Supported by grants from the Key Program of the National Natural Science Foundation of China (82130093), Shanghai Municipal Science and Technology Major Project (ZD2021CY001), Hunan Provincial Innovative Construction Special Fund: Emergency response to COVID-19 outbreak (No. 2020SK3012), and Chinese Academy of Medical Sciences Coronavirus Disease 2019 Science and Technology Research Project in 2020 (No. 2020HY320003).

**doi:** 10.46234/ccdcw2023.011

[#] Corresponding authors: Shixiong Hu, 379788967@qq.com; Hongjie Yu, yhj@fudan.edu.cn.

[1] Hunan Provincial Center for Disease Control and Prevention;Workstation for Emerging Infectious Disease Control and Prevention, Chinese Academy of Medical Sciences, Changsha City, Hunan Province, China; [2] Shanghai Institute of Infectious Disease and Biosecurity, Fudan University, Shanghai Municipality, China; [3] School of Public Health, Fudan University, Key Laboratory of Public Health Safety, Ministry of Education, Shanghai Municipality, China; [4] Division of International Epidemiology and Population Studies, Fogarty International Center, National Institutes of Health, Bethesda, MD, USA; [5] Laboratory of Computational Epidemiology and Public Health, Department of Epidemiology and Biostatistics, Indiana University School of Public Health, Bloomington, IN, USA.
[&] Joint first authors.

Submitted: November 01, 2022; Accepted: January 03, 2023

## REFERENCES

1. Hu SX, Wang W, Wang Y, Litvinova M, Luo KW, Ren LS, et al. Infectivity, susceptibility, and risk factors associated with SARS-CoV-2 transmission under intensive contact tracing in Hunan, China. Nat Commun 2021;12(1):1533. http://dx.doi.org/10.1038/s41467-021-21710-6.
2. Office of Changde Municipal People's Government. An asymptomatic case was reported in Changde City, Hunan Province. https://www.changde.gov.cn/cdzx/cdyw/content_850758. [2022-7-26].

3. Kang M, Xin HL, Yuan J, Ali ST, Liang ZM, Zhang JY, et al. Transmission dynamics and epidemiological characteristics of SARS-CoV-2 Delta variant infections in Guangdong, China, May to June 2021. Euro Surveill 2022;27(10):2100815. http://dx.doi.org/10.2807/1560-7917.ES.2022.27.10.2100815.
4. Ogata T, Tanaka H, Irie F, Hirayama A, Takahashi Y. Shorter incubation period among unvaccinated delta variant coronavirus disease 2019 patients in Japan. Int J Environ Res Public Health 2022;19(3):1127. http://dx.doi.org/10.3390/IJERPH19031127.
5. Del Águila-Mejía J, Wallmann R, Calvo-Montes J, Rodríguez-Lozano J, Valle-Madrazo T, Aginagalde-Llorente A. Secondary attack rate, transmission and incubation periods, and serial interval of SARS-CoV-2 omicron variant, spain. Emerg Infect Dis 2022;28(6):1224 – 8. http://dx.doi.org/10.3201/eid2806.220158.
6. Manica M, Litvinova M, De Bellis A, Guzzetta G, Mancuso P, Vicentini M, et al. Estimation of the incubation period and generation time of SARS-CoV-2 Alpha and Delta variants from contact tracing data. Epidemiol Infect 2022. https://doi.org/10.1017/S0950268822001947.
7. Hart WS, Miller E, Andrews NJ, Waight P, Maini PK, Funk S, et al. Generation time of the alpha and delta SARS-CoV-2 variants: an epidemiological analysis. Lancet Infect Dis 2022;22(5):603 – 10. http://dx.doi.org/10.1016/S1473-3099(22)00001-9.
8. Park SW, Sun KY, Champredon D, Li M, Bolker BM, Earn DJD, et al. Forward-looking serial intervals correctly link epidemic growth to reproduction numbers. Proc Natl Acad Sci USA 2021;118(2): e2011548118. http://dx.doi.org/10.1073/pnas.2011548118.
9. Riley S, Wang HW, Eales O, Haw D, Walters CE, Ainslie KEC, et al. REACT-1 round 12 report: resurgence of SARS-CoV-2 infections in England associated with increased frequency of the Delta variant. medRxiv 2021. http://medrxiv.org/content/early/2021/06/21/2021.06.17.21259103.abstract.
10. Kang M, Yi Y, Li Y, Sun LM, Deng AP, Hu T, et al. Effectiveness of inactivated COVID-19 vaccines against illness caused by the B. 1.617.2 (Delta) variant during an outbreak in Guangdong, China: a cohort study. Ann Intern Med 2022;175(4):533 – 40. http://dx.doi.org/10.7326/M21-3509.
11. Chen XH, Yan XM, Sun KY, Zheng N, Sun RJ, Zhou JX, et al. Estimation of disease burden and clinical severity of COVID-19 caused by Omicron BA.2 in Shanghai, February-June 2022. Emerg Microbes Infect 2022;11(1):2800-7. http://dx.doi.org/10.1080/22221751.2022.2128435.
12. Chen ZY, Deng XW, Fang LQ, Sun KY, Wu YP, Che TL, et al. Epidemiological characteristics and transmission dynamics of the outbreak caused by the SARS-CoV-2 Omicron variant in Shanghai, China: a descriptive study. Lancet Reg Health West Pacific 2022;29:100592. http://dx.doi.org/10.1016/j.lanwpc.2022.100592.
13. Bager P, Wohlfahrt J, Bhatt S, Stegger M, Legarth R, Møller CH, et al. Risk of hospitalisation associated with infection with SARS-CoV-2 omicron variant versus delta variant in Denmark: an observational cohort study. Lancet Infect Dis 2022;22(7):967 – 76. http://dx.doi.org/10.1016/S1473-3099(22)00154-2.

# Supplementary Material

## The GLMM Model

We performed a generalized linear mixed-effects model (GLMM) to quantify the effects of potential drivers of susceptibility and infectivity of the Delta variant. The GLMM was conducted based on the contact data, where each contact was epidemiologically linked to at least one potential infector. For a contact who had interacted with more than one SARS-CoV-2 infected person, we chose the first infected individuals they had been exposed to as the potential infector in our main analysis. If they had been exposed to multiple individuals at the same time, we randomly chose one from among these infectors as the potential infector. The specifications of the GLMM models were defined as follows:

$$g(u_i) = \alpha + \beta_1 Age\_Vaccination\_infector_i + \beta_2 Age\_Vaccination\_contact_i + \beta_3 Contact\_type_i + \beta_4 Sex\_infector_i + \beta_5 Sex\_contact_i + u_{0i}$$

where:

· $g$ is a logit link function;

· $\alpha$ is the intercept;

· $Age\_Vaccination\_infector_i$ is the fixed-effect of the age group and vaccination status of the infector in the successful (1) or unsuccessful (0) transmission event $i$;

· $Age\_Vaccination\_contact_i$ is the fixed-effect of the age group and vaccination status of the contact (potential infectee) in the successful/unsuccessful transmission event $i$;

· $Contact\_type_i$ is the type of contact that occurred in the successful/unsuccessful transmission event $i$;

· $Sex\_infector_i$ is the sex of the infector in the successful/unsuccessful transmission event $i$;

· $Sex\_contact_i$ is the sex of the contact in the successful/unsuccessful transmission event $i$;

· $u_{0i}$ is the random effect.

To evaluate the robustness of the regression estimates against the uncertainties in the source of the exposures, we repeated the regression analysis 1,000 times, where the potential infectors were randomly chosen from multiple infectors of contacts in each stochastic realization, regardless of the time order of exposure. We reported the mean and the 2.5–97.5th percentiles of the point estimates of the variables of interest, i.e., the age and vaccination status of both the infectors and contacts, based on all regression results from 1,000 stochastic realizations. The results are reported in Supplementary Table S4.

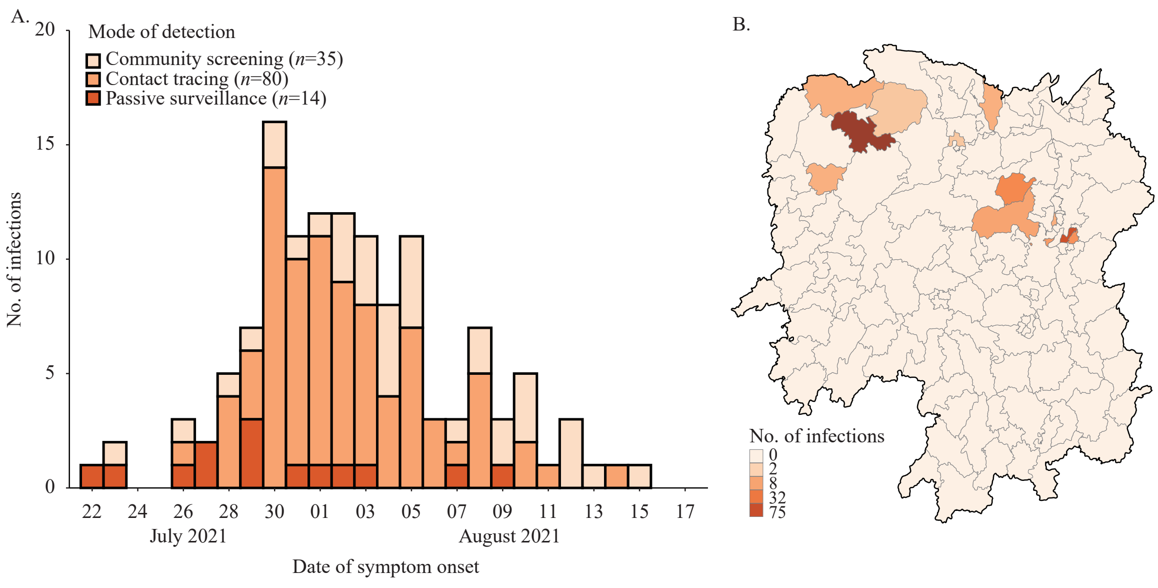


SUPPLEMENTARY FIGURE S1. Spatiotemporal distributions of SARS-CoV-2 Delta infections in Hunan Province, China, 2021. (A). Daily number of new infections by the date of symptom onset and the mode of detection. (B). Spatial distribution of infected individuals in each city of Hunan Province.

Note: For the asymptomatic infections and confirmed cases diagnosed by imaging characteristics, we substituted the date of the first positive specimen taken for the date of symptom onset.

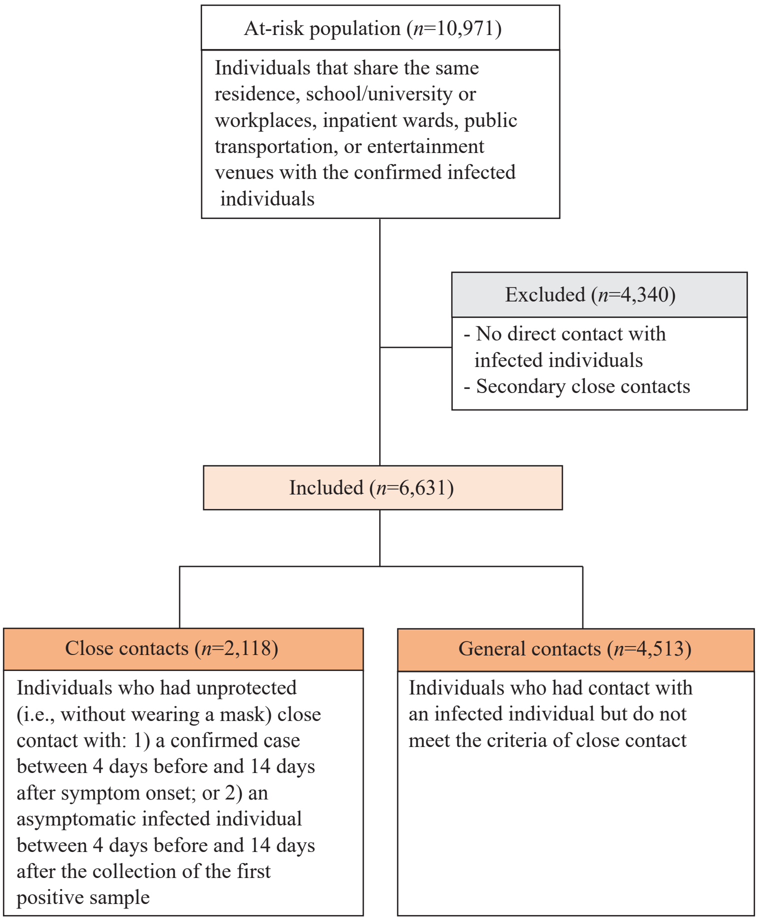


SUPPLEMENTARY FIGURE S2. The flowchart of the selection of study participants.

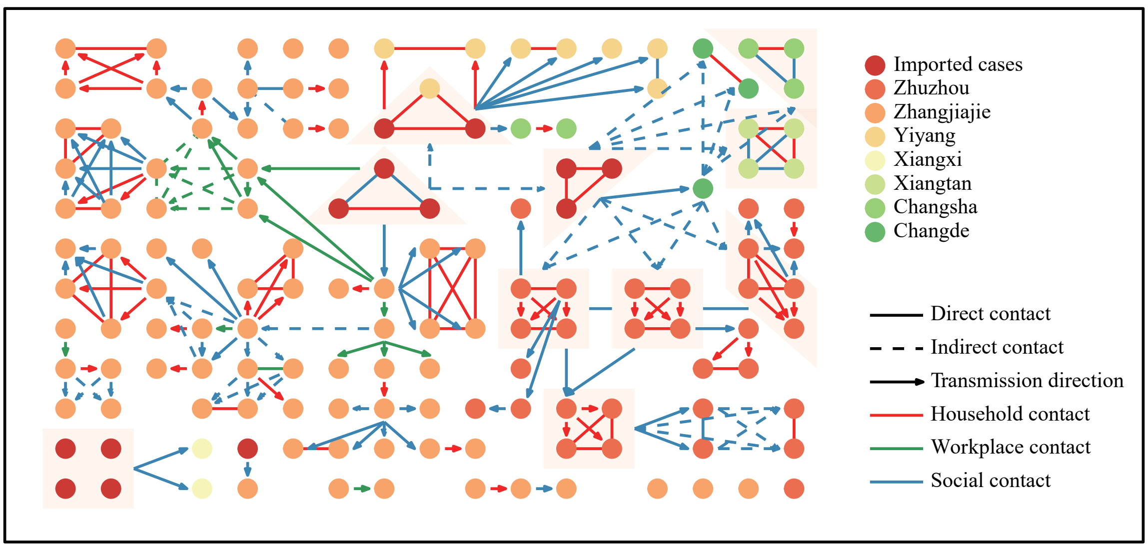


SUPPLEMENTARY FIGURE S3. Epidemiological transmission network of severe acute respiratory syndrome coronavirus 2 (SARS-CoV-2) Delta transmission in Hunan Province, China.

Note: A total of 13 infected visitors and 129 local infections are shown in the network, indicated by the dots. The lines and arrows indicate potential transmission routes. Direct contact refers to unprotected close contact with a confirmed SARS-CoV-2 infection. Indirect contact refers to potential contact with a confirmed SARS-CoV-2 infection through sharing the same residential communities, study or workplaces, inpatient wards, public transportation, or entertainment venues.

SUPPLEMENTARY TABLE S1. The completeness of the variables for SARS-CoV-2 Delta infections and the at-risk population.

| Variables | Percentage of infections, % (*n*=129) | Percentage of risk population, % (*n*=10,971) |
|---|---|---|
| Demographic information | | |
| Age | 100 (129/129) | 96.5 (10,586/10,971) |
| Sex | 100 (129/129) | 97.3 (10672/10,971) |
| Vaccination information | | |
| Vaccine manufacturer (1st dose) | 100 (67/67) | 100 (6,724/6,724) |
| Vaccination date (1st dose) | 100 (67/67) | 100 (6,723/6,724) |
| Vaccine manufacturer (2nd dose) | 100 (44/44) | 100 (5,348/5,348) |
| Vaccination date (2nd dose) | 100 (44/44) | 100 (5,348/5,348) |
| Vaccine manufacturer (3rd dose)* | 100 (1/1) | 100 (604/604) |
| Vaccination date (3rd dose) | 100 (1/1) | 100 (604/604) |
| Exposure information | | |
| Exposure start date | 74.4 (96/129) | 56.1 (6,152/10,971) |
| Exposure end date | 80.6 (104/129) | 88.6 (9,716/10,971) |
| Contact type | 100 (129/129) | 92.1 (10,102/10,971) |
| Clinical information | | |
| Date of symptom onset | 83.6 (92/110) | − |
| Date of the first positive sample collection for PCR testing | 100 (129/129) | − |
| Date of the laboratory confirmation | 100 (129/129) | − |
| Clinical severity | 100 (129/129) | − |
| Type of detection | 100 (129/129) | − |

Note: "−" means data not available.
Abbreviation: SARS-CoV-2=severe acute respiratory syndrome coronavirus 2; COVID-19=coronavirus disease 2019.
* The three-dose regimen of a tandem-repeat dimeric RBD protein-based COVID-19 vaccine ZF2001 was selected for use in real-world practice.

SUPPLEMENTARY TABLE S2. Estimates of the incubation period and serial interval.

| Distribution | Sample size for estimation | Parameters [mean (SD)] | Mean (days) | Quantiles (0.025–0.975, days) | AIC |
|---|---|---|---|---|---|
| Incubation period | | | | | |
| Gamma | 71 | shape=3.02(0.60), rate=0.57(0.12) | 5.3 | 1.1–12.9 | 217.9 |
| Weibull | 71 | shape=1.69(0.17), scale=5.94(0.49) | 5.3 | 0.6–12.8 | 222.4 |
| Log-normal | 71 | meanlog=1.50(0.08), sdlog=0.58(0.06) | 5.3 | 1.5–13.9 | 216.3 |
| Serial interval | | | | | |
| Gamma | 54 | shape=6.09(1.17), rate=0.59(0.12), shift=6 | 4.3 | −2.2–14.0 | 274.5 |
| Weibull | 54 | shape=3.12(0.34), scale=11.52(0.53), shift=6 | 4.3 | −2.4–11.5 | 265.7 |
| Log-normal | 54 | meanlog=2.25(0.07), sdlog=0.47(0.05), shift=6 | 4.6 | −2.2–18.0 | 288.0 |

Abbreviation: SD=standard deviation; AIC=Akaike information criterion.

SUPPLEMENTARY TABLE S3. A sensitivity analysis of GLMM-logit regression projecting uncertainties of the fixed-effects of age (years) and vaccination status induced by those contacts with multiple infectors.

| Age and vaccination status | Susceptibility odds ratio* | | Transmissibility odds ratio* | |
|---|---|---|---|---|
| | Mean | (Quantiles, 0.025–0.975th) | Mean | (Quantiles, 0.025–0.975th) |
| Unvaccinated children (0–9 years) | 2.13 | (1.79, 2.57) | 1.34 | (0.52, 2.78) |
| Unvaccinated adolescents (10–17 years) | 1.29 | (1.04, 1.58) | 0.72 | (0.38, 1.19) |
| Unvaccinated adults (18–64 years) | Reference | | Reference | |
| Vaccinated adults (18–64 years) | 0.47 | (0.41, 0.52) | 0.59 | (0.35, 0.95) |

Note: All children and adolescents (under 18 years) were unvaccinated, as they were not covered by the COVID-19 vaccination program in the Chinese mainland during the Delta outbreak. Vaccinated adults denote fully vaccinated adults, while partially vaccinated adults were deemed unvaccinated adults in the analysis. Contacts who were aged at or over 65 years or whose infectors were aged at or over 65 years were excluded from this analysis due to the small sample size.

* The GLMM-logit regression was repeated 1,000 times, where one single infector was randomly chosen for those contacts with multiple infectors in each stochastic realization. The mean odds ratio and 2.5–97.5th percentiles were summarized based on all results from 1,000 stochastic realizations. The odds ratios of age and vaccination status were adjusted by contact setting and the sex of the infector and contact.

SUPPLEMENTARY TABLE S4. Estimating the association of potential risk factors with the risk of acquiring and transmitting the SARS-CoV-2 Delta variant based on 6,135 contacts in Hunan, China.

| Characteristic | Multivariate analysis | |
|---|---|---|
| | *OR* (95% *CI*) | *P* value |
| Age (years) and vaccination status of contacts† | | |
| Unvaccinated children (0–9 years) | 2.40 (1.12, 5.18) | 0.025** |
| Unvaccinated adolescents (10–17 years) | 1.38 (0.59, 3.25) | 0.458 |
| Unvaccinated adults (18–64 years) | Reference | |
| Vaccinated adults (18–64 years) | 0.54 (0.29, 0.99) | 0.048* |
| Age (years) and vaccination status of infectors§ | | |
| Unvaccinated children (0–9 years) | 2.19 (0.52, 9.23) | 0.285 |
| Unvaccinated adolescents (10–17 years) | 1.29 (0.31, 5.39) | 0.728 |
| Unvaccinated adults (18–64 years) | Reference | |
| Vaccinated adults (18–64 years) | 0.92 (0.32, 2.65) | 0.875 |
| Type of contact | | |
| Household contacts | 6.90 (3.24, 14.68) | <0.001*** |
| Health care | 0.29 (0.06, 1.34) | 0.113 |
| Social contact | Reference | |
| Workplace contact | 0.58 (0.13, 2.50) | 0.461 |
| Other close contact | 0.04 (0.01, 0.14) | <0.001*** |
| General contact | 0.10 (0.05, 0.21) | <0.001*** |
| Sex of contacts | | |
| Female | Reference | |
| Male | 0.68 (0.41, 1.13) | 0.138 |
| Sex of infectors | | |
| Female | Reference | |
| Male | 0.42 (0.16, 1.10) | 0.078 |

Note: All children and adolescents (under 18 years) were unvaccinated, as they were not covered by the COVID-19 vaccination program in mainland China during the Delta outbreak. Vaccinated adults denote fully vaccinated adults, while partially vaccinated adults were deemed unvaccinated adults in the analysis.

Abbreviation: *CI*=confidence interval; *OR*=odds ratio.

* *P*<0.05;

** *P*<0.01;

*** *P*<0.001;

† Contacts who were aged at or over 65 years or whose infectors were aged at or over 65 years were excluded from this analysis due to the small sample size.

§ For a contact who had interacted with more than one SARS-CoV-2 infection, we chose the first infected individuals they had been exposed to as the potential infector. If they had been exposed to multiple infectors at the same time, we randomly chose one from among these infectors as the potential infector.

Review

# Measurement of Non-Steady Noise and Assessment of Occupational Hearing Loss Based on the Temporal Structure of Noise

Meibian Zhang[1,#]; Anke Zeng[1]; Jiarui Xin[1]; Xiangjing Gao[2]; Wei Qiu[3]; Xin Sun[1]

Noise-induced hearing loss (NIHL) has become a global public health problem, and the economic burden of hearing loss caused by noise exposure accounts for 19.6% of the economic burden of all risk factors in the workplace (*1*). The prevalence of occupational NIHL was estimated to be 10% in relevant occupational population in developed countries and 17%–39% (e.g., textile and petrochemical industries), and 53%–67% (e.g., cement and automobile industries) in developing countries in Asia, respectively. (*2*). In China, occupational noise-induced deafness has become the second primary occupational disease after pneumoconiosis, with the number of reported cases increasing at an average annual rate of 18.68% from 2010 to 2019 (*3–4*). The prevalence of occupational NIHL in the Chinese occupational population was 21.3%, of which 30.2% was related to high-frequency NIHL (an early sign of NIHL) (*2*).

Controlling the risk of hearing loss is critical for protecting workers' hearing health and noise exposure measurement and assessment are crucial links within these efforts. At present, workers are often widely exposed to non-steady noise in occupational environments (*5*). The important difference between steady-state and non-steady noise is the energy distribution (temporal structure), i.e., the former is statistically normal, and the latter is non-normal and time-varying. Animal and human data show that the temporal structure of noise is a risk factor for NIHL (*6*). Presently, applying noise's temporal structure to quantitative measurement and evaluation of industrial noise has made some progress, but there are few reports on the relevant review. The aim of present paper is thus to review the research progress of measuring and assessing workplace non-steady noise based on the temporal structure of noise.

## Identification of Non-Steady Noise Based on Temporal Structure

This study's definition of non-steady noise is defined as transient high-energy impulsive noise superimposed on Gaussian background noise (*5,7*), which differs from the traditional definition (based on noise energy). In the traditional definition, non-steady noise is noise with a fluctuation greater than 3dB(A) determined by the sound level meter with a "slow" dynamic characteristic during the measuring time (*8–9*), which fails to reflect the temporal structure of non-steady noise.

Measuring the following parameters for the temporal structure of single impulse noise is usually standard when evaluating noise: peak pressure, interpeak interval, and pulse duration (*10*). Kurtosis, sensitive to and primarily determined by these three above variables, can quantify the impulsiveness of complex noise and is much more practical as a specific metric for the temporal structure of complex noise (*6,11–12*). It can quantify the noise signal's complexity (*6,13*).

Kurtosis is a statistical measure of extreme values or outliers relative to a normal distribution (*11*). The calculation formula is following:

$$\beta = \frac{\frac{1}{n}\sum_{i=1}^{n}(x_i - \bar{x})^4}{\left[\frac{1}{n}\sum_{i=1}^{n}(x_i - x)^2\right]^2} \quad (1)$$

where β is the kurtosis, $x_i$ is the $i^{th}$ value of noise amplitude, and $\bar{x}$ is the sample mean. Kurtosis describes the tendency for a sound to have high amplitude events that depart substantially from underlying, continuous, steady-state noise. It should be noted that kurtosis has high sampling variability since the length of intervals over which kurtosis is determined can affect the outcome (*14–15*). In practice, the kurtosis of the recorded noise signal is usually computed over consecutive 60-second time windows (without overlap) over the whole measurement duration using a sampling rate of 48 kHz for noise recordings (*16*).

Figure 1A shows a sample of a steady-state noise, i.e., a flat waveform with a kurtosis value of 3.

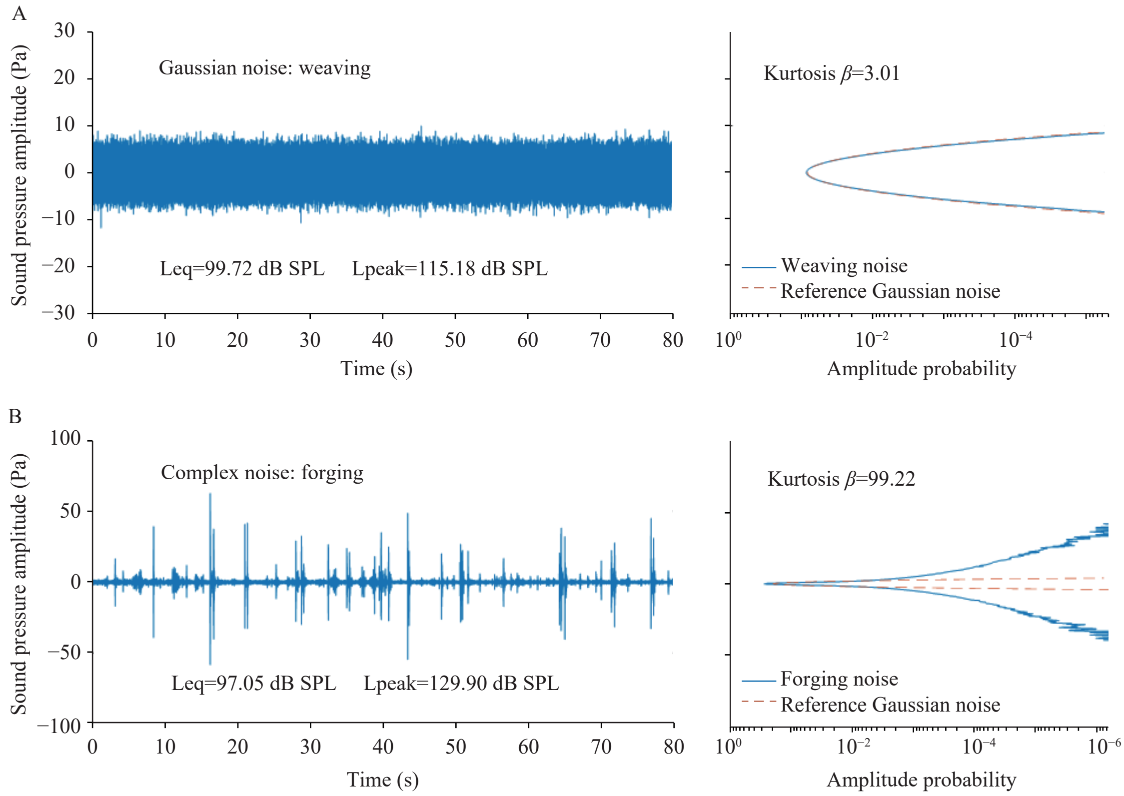


FIGURE 1. Waveforms (left) and amplitude probabilities (right) from two industrial noises: (A) steady-state noise; (B) non-steady (complex) noise. Red lines, background Gaussian noise probabilities.
Abbreviation: Leq=equivalent sound pressure level; Lpeak=peak sound pressure level; SPL=sound pressure level.

Figure 1B illustrates an example of a non-steady noise, i.e., a Gaussian background noise punctuated by a temporally complex series of randomly occurring, high-level, impulsive/impact noise transients. The noise waveform and kurtosis of different work types are unique, providing a practical approach for identifying different types of industrial noise (*6*).

## A Need for Modification to Existing Noise Standards Based on Kurtosis

The international noise exposure standards [e.g., ISO 1999: 2013, ISO 9612 (2009), HSE 2005 and NIOSH 1998] and China's noise exposure measurement standard (GBZ/T 189.8) are based on the "equal energy hypothesis (EEH)" (*9,17–20*). The energy of the noise (e.g., equivalent continuous A-weighted sound pressure level, $L_{Aeq}$) is considered the only measurement and evaluation criterion. $L_{Aeq}$ is normalized to a nominal 8-hour working day ($L_{EX,8\ h}$) or a nominal week of five 8 h working days ($L_{EX,40\ h}$). However, due to the "peak clipping effect" (i.e., a clip of instrument electronics against high input levels greater than 130 dB and a lacking of a fast enough time constant to capture impulses) for noise with impulsive components, the $L_{Aeq}$ measurement technique using noise dosimeter or sound level meter can not reflect the temporal structure of noise and can not capture the peak change (*21*).

In the existing standards, LAeq serves as the sole metric when evaluating NIHL based on the EEH. The EEH assumes that hearing loss caused by noise exposure is proportional to the exposure duration multiplied by the energy intensity, thus implying that hearing loss is independent of the acoustic energy temporal distribution. The problem with the existing standards is that the temporal characteristic of non-Gaussian noise is not taken into account when assessing the effects of noise on hearing. As a result, non-steady noise measurement (especially for noise with a high kurtosis value) is inaccurate, and hearing loss is underestimated when applying the existing standards. Epidemiological data showed that the current ISO 1999 prediction model underestimated the complex noise-induced permanent threshold shift (NIPTS) by over 10 dB HL on average (*6,14–15,22*); The 85 dB(A) noise exposure limit may still be unsafe due to noises with high kurtosis values (*6*). Therefore, it is necessary to apply kurtosis to adjust the energy level in order to more effectively assess NIHL.

## The Role of Kurtosis in Evaluating NIHL

Previous animal studies have found that kurtosis can distinguish the degree of hearing loss caused by different temporal structural noises under the same noise exposure level (*13,23*). These findings have been confirmed by subsequent epidemiological survey data (*24–25*). Human evidence demonstrates that the temporal structure of noise is a risk factor for occupational NIHL, in addition to noise level, exposure duration, age, and sex (*6,26–27*). Complex noise induces more serious hearing damage among workers than steady-state noise [odds ratio (*OR*)=2.20, 95% confidence interval (*CI*): 1.78–2.72] (*26*). Kurtosis had a significant dose-effect relationship with the prevalence of high-frequency NIHL (*6,28*). $NIPTS_{346}$ increased with kurtosis across different cumulative noise exposure (CNE) levels. The notch degree of hearing loss at the high frequencies 3, 4, and 6 kHz deepened with the increase of kurtosis and reached its maximum at 4 kHz (*6,28*). The underestimation of NIPTS by the ISO 1999 prediction model increases with the increase of kurtosis level (*28*). Thus, the permissible exposure limit of 85 dB(A) may not be safe, as non-steady noise with a high kurtosis value can aggravate or accelerate early NIHL (*6*). These data reveal that the kurtosis metric is an adjunct to noise energy for qualifying and assessing non-steady noise in the workplace.

## Methodologies of Applying Kurtosis to Adjust Noise Energy

Currently, there are two adjustment protocols, one is to adjust the noise exposure level (e.g., $L_{EX,8\ h}$ or $L_{EX,40\ h}$) (*6,28*), and another is to adjust the exposure duration in CNE (*6,28–31*). However, due to the ambiguity of the relationship between CNE and NIPTS, and the uncertainty of exposure duration for workers whose jobs change frequently, it is not recommended to adjust the exposure duration in CNE in practice. Instead, an adjustment protocol for noise intensity is preferable (*28*).

The adjustment protocol applies kurtosis to adjust the noise intensity based on Goley's protocol from animal data (*32*). The formula is as follows:

$$L_{EX,8\ h}\text{-K}=L_{EX,8\ h} + \lambda \times \lg(\beta_N/3) \qquad (2)$$

In the formula, $\beta_N$ is the kurtosis value of the noise measured; $L_{EX,8\ h}$-K is kurtosis-adjusted $L_{EX,8\ h}$; and λ is the adjustment coefficient obtained from the dose-effect relationship between noise exposure and hearing loss. The λ value is recommended as 6.5 based on human data (*6,28*). The $L_{EX,8\ h}$-K can be calculated as follows:

$$L_{EX,8\ h}\text{-K}=L_{EX,8\ h} + 6.5 \times \lg(\beta_N/3) \qquad (3)$$

where $\beta_N$ is the average kurtosis value of noise during measurement duration. For example, when $\beta_N$ is 30, the $L_{EX,8\ h}$ or $L_{EX,40\ h}$ increases by 6.5 dB(A). After the adjustment of $L_{EX,8\ h}$ by kurtosis, this study found that the underestimation of $NIPTS_{346}$ by *ISO 1999* improved significantly (less than 1.23 dB HL) (*6*).

Currently, *ISO 1999:2013 "Acoustics-Estimation of Noise-Induced Hearing Loss"* is being revised based on the adjusting protocol. The National Institute of Occupational Health and Poisoning Control: Chinese Center for Disease Control and Prevention is carrying out the preliminary research project "*Kurtosis Based Occupational Noise Exposure Limit and Measurement Standard Revision*" on occupational health standards.

## Developing a Measurement Guideline Based on Kurtosis Adjustment

A dedicated personal sound exposure meter (or noise dosimeter) should be developed to have at least one of the following functions: 1) sound recording for further analysis of kurtosis or $L_{Aeq}$; or 2) automatic calculation of kurtosis, $L_{EX,8\ h}$, or $L_{EX,8\ h}$-K for direct reading. A dosimeter prototype with kurtosis function has been successfully developed in China. The direct reading method of kurtosis and $L_{EX,8\ h}$-K values is preferred if the dosimeter with kurtosis function becomes commercially available (*28*).

The measurement guideline for non-steady noise can be developed based on modifying existing standards, e.g., the *ISO 9612 (2009)*. Measurement procedures may include the following items: field investigation, preparation of instruments, determination of sampling subjects, dosimeter wearing, noise waveform analysis, or direct reading of the device, data analysis, measurement records, and notes of non-steady noise measurements. The condition of using kurtosis adjustment (Formula 3) in the assessment of NIHL is $L_{EX,8\ h}$ between 70 and 95 dB(A). For $L_{EX,8\ h}$ higher than 95 dB(A), Formula 3 provides a reasonable interpolation (*28*).

## Outlook

Non-steady noise is the primary type of noise in the workplace. Existing noise measurement and evaluation standards are not fully applicable to non-steady noise. As a sensitive temporal structural index for non-steady noise exposure, kurtosis can be used as an adjunct parameter of the noise energy to evaluate occupational hearing loss more effectively. The following measures are thus recommended for further research.

1) Further developing and improving the database on the noise-exposed population through large-scale and well-designed epidemiological investigations. The database should cover noise exposure data with different kurtosis levels and include different noise-hazard industries and their main types of work. In addition, it is also necessary to develop databases on the statistical distribution of hearing threshold levels from the general population in Asian countries.

2) Methodological studies applying kurtosis to adjust noise intensity. More population epidemiological data are needed to verify the applicability and effectiveness of the new parameter of the noise intensity adjusted by kurtosis in assessing occupational hearing loss.

3) Revisions of the measurement and assessment standards for occupational noise. The population data can reconstruct the dose-response (effect) relationship based on the kurtosis adjustment, which is critical for revising existing noise exposure standards. In addition, a dedicated personal sound exposure meter (or noise dosimeter) with a function of waveform analysis or direct reading for kurtosis and $L_{EX,8\ h}$-K (or $L_{EX,40\ h}$-K) needs to be further commercialized and available.

4) Studies on the influence of noise's temporal structure on principal characteristics of occupational hearing loss. These affected characteristics may include the notching phenomenon of high-frequency hearing threshold, the maximum hearing threshold shift at different frequencies, and the onset period or latency of hearing loss related to exposure duration. Strengthening study of the principal characteristics of occupational hearing loss related to the temporal structure of noise is critical for the diagnosis and early prevention of NIHL or noise-induced deafness and for improving the hearing protection plan of workers.

**Funding:** This work was supported by the National Key R&D Program of China (2022YFC2503200, 2022YFC2503203); the Pre-research project on occupational health standards (20210102); and the National Institutes of Health, National Institute on Deafness and Other Communication Disorders, United States (1R01DC015990).

**doi:** 10.46234/ccdcw2023.012

# Corresponding author: Meibian Zhang, zhangmb@niohp.chinacdc.cn.

[1] National Institute of Occupational Health and Poison Control, Chinese Center for Disease Control and Prevention, Beijing Municipality, China; [2] Occupational Health and Radiation Protection Institute, Zhejiang Provincial Center for Disease Control and Prevention, Hangzhou City, Zhejiang Province, China; [3] Zhejiang Lab, Hangzhou City, Zhejiang Province, China.

Submitted: November 20, 2022; Accepted: January 16, 2023

## REFERENCES

1. GBD 2016 Occupational Risk Factors Collaborators. Global and regional burden of disease and injury in 2016 arising from occupational exposures: a systematic analysis for the Global Burden of Disease Study 2016. Occup Environ Med 2020;77(3):133 – 41. http://dx.doi.org/10.1136/oemed-2019-106008.
2. Zhou JN, Shi ZH, Zhou LF, Hu Y, Zhang MB. Occupational noise-induced hearing loss in China: a systematic review and meta-analysis. BMJ Open 2020;10(9):e039576. http://dx.doi.org/10.1136/bmjopen-2020-039576.
3. Sun X. Occupational noise exposure and worker’s health in China. China CDC Wkly 2021;3(18):375 – 77. http://dx.doi.org/10.46234/ccdcw2021.102.
4. Chen YL, Zhang MB, Qiu W, Sun X, Wang X, Dong YW, et al. Prevalence and determinants of noise-induced hearing loss among workers in the automotive industry in China: a pilot study. J Occup Health 2019;61(5):387 – 97. http://dx.doi.org/10.1002/1348-9585.12066.
5. Suter AH. Occupational hearing loss from non-Gaussian noise. Semin Hear 2017;38(3):225 – 62. http://dx.doi.org/10.1055/s-0037-1603726.
6. Zhang MB, Qiu W, Xie HW, Xu XH, Shi ZH, Gao XJ, et al. Applying kurtosis as an indirect metric of noise temporal structure in the assessment of hearing loss associated with occupational complex noise exposure. Ear Hear 2021;42(6):1782 – 96. http://dx.doi.org/10.1097/AUD.0000000000001068.
7. Hamernik RP, Qiu W. Energy-independent factors influencing noise-induced hearing loss in the chinchilla model. J Acoust Soc Am 2001;110(6):3163 – 8. http://dx.doi.org/10.1121/1.1414707.
8. Ministry of Health of the People's Republic of China. GBZ 2.2-2007 Occupational exposure limits for hazardous agents in the workplace, Part 2: Physical agents. Beijing: People's Medical Publishing House, 2007. (In Chinese).
9. Ministry of Health of the People's Republic of China. GBZ/T 189.8-2007 Measurement of physical agents in workplace, Part 8: Noise. Beijing: Standards Press of China, 2007. (In Chinese).
10. Henderson D, Hamernik RP. Impulse noise: critical review. J Acoust Soc Am 1986;80(2):569 – 84. http://dx.doi.org/10.1121/1.394052.
11. Qiu W, Zhang MB, Hu WJ, Sun X. Application of the kurtosis metric to the assessment of hearing loss associated with occupational noise exposure. China CDC Wkly 2021;3(18):390 – 93. http://dx.doi.org/10.46234/ccdcw2021.105.
12. Qiu W, Hamernik RP, Davis RI. The value of a kurtosis metric in estimating the hazard to hearing of complex industrial noise exposures. J Acoust Soc Am 2013;133(5):2856 – 66. http://dx.doi.org/10.1121/1.4799813.
13. Müller RAJ, Von Benda-Beckmann AM, Halvorsen MB, Ainslie MA. Application of kurtosis to underwater sound. J Acoust Soc Am 2020;148(2):780. http://dx.doi.org/10.1121/10.0001631.
14. Zhang MB, Hu Y, Qiu W, Gao XJ, Zeng AK, Shi ZH, et al. Developing a guideline for measuring workplace non-Gaussian noise exposure based on kurtosis adjustment of noise level in China. Front Public Health 2022;10:1003203. http://dx.doi.org/10.3389/fpubh.2022.1003203.
15. Zhang MB, Gao XJ, Murphy WJ, Kardous CA, Sun X, Hu WJ, et al.

Estimation of occupational noise-induced hearing loss using kurtosis-adjusted noise exposure levels. Ear Hear 2022;43(6):1881 – 92. http://dx.doi.org/10.1097/AUD.0000000000001223.
16. Tian Y, Ding WX, Zhang MB, Zhou TS, Li JS, Qiu W. Analysis of correlation between window duration for kurtosis computation and accuracy of noise-induced hearing loss prediction. J Acoust Soc Am 2021;149(4):2367 – 76. http://dx.doi.org/10.1121/10.0003954.
17. ISO (International Standard Organization). ISO 1999:2013. Acoustics-estimation of noise-induced hearing loss. Geneva, Switzerland: International Organization for Standardization, 2013. https://www.iso.org/standard/45103.html.
18. International Standard Organization (ISO). ISO 1999:1990. Acoustics-determination of occupational noise exposure and estimation of noise-induced hearing impairment. Geneva, Switzerland: International Organization for Standardization, 2013. https://www.iso.org/standard/6759.html.
19. HSE (Health and Safety Executive). The control of noise at work regulations 2005: guidance on regulations. UK: HSE; 2005. HMSO PublicationNo1643. https://www.legislation.gov.uk/uksi/2005/1643/contents/made.
20. National Institute for Occupational Safety and Health (NIOSH). Criteria for a recommended standard: occupational noise exposure. Cincinnati: NIOSH; 1998. DHHS (NIOSH) Publication No. 98-126. https://www.cdc.gov/niosh/docs/98-126/pdfs/98-126.pdf?id=10.26616/NIOSHPUB98126.
21. Davis RR, Clavier O. Impulsive noise: a brief review. Hear Res 2017;349:34 – 6. http://dx.doi.org/10.1016/j.heares.2016.10.020.
22. Lempert B. ISO estimates of noise-induced hearing impairment. J Acoust Soc Am 2019;145(6):3640. http://dx.doi.org/10.1121/1.5111862.
23. Hamernik RP, Qiu W, Davis B. The effects of the amplitude distribution of equal energy exposures on noise-induced hearing loss: the kurtosis metric. J Acoust Soc Am 2003;114(1):386 – 95. http://dx.doi.org/10.1121/1.1582446.
24. Davis RI, Qiu W, Hamernik RP. Role of the kurtosis statistic in evaluating complex noise exposures for the protection of hearing. Ear Hear 2009;30(5):628 – 34. http://dx.doi.org/10.1097/AUD.0b013e3181b527a8.
25. Zhang MB, Xie HW, Zhou JN, Sun X, Hu WJ, Zou H, et al. New metrics needed in the evaluation of hearing hazard associated with industrial noise exposure. Ear Hear 2021;42(2):290 – 300. http://dx.doi.org/10.1097/AUD.0000000000000942.
26. Shi ZH, Zhou JN, Huang YW, Hu Y, Zhou LF, Shao YQ, et al. Occupational hearing loss associated with non-Gaussian noise: a systematic review and meta-analysis. Ear Hear 2021;42(6):1472 – 84. http://dx.doi.org/10.1097/AUD.0000000000001060.
27. Zhou LF, Ruan XY, Wang TS, Xie HW, Hu Y, Shi ZH, et al. Epidemiological characteristics of hearing loss associated with noise temporal structure among manufacturing workers. Front Integr Neurosci 2022;16:978213. http://dx.doi.org/10.3389/fnint.2022.978213.
28. Zhang MB, Gao XJ, Qiu W, Sun X, Hu WJ. The role of the kurtosis metric in evaluating the risk of occupational hearing loss associated with complex noise — Zhejiang Province, China, 2010-2019. China CDC Wkly 2021;3(18):378 – 82. http://dx.doi.org/10.46234/ccdcw2021.103.
29. Shi ZH, Wang X, Gao XJ, Xie HW, Zhou LF, Zhang MB. Assessment of occupational hearing loss associated with non-Gaussian noise using the kurtosis-adjusted cumulative noise exposure metric: a cross-sectional survey. Front Psychol 2022;13:870312. http://dx.doi.org/10.3389/fpsyg.2022.870312.
30. Xie HW, Qiu W, Heyer NJ, Zhang MB, Zhang P, Zhao YM, et al. The use of the kurtosis-adjusted cumulative noise exposure metric in evaluating the hearing loss risk for complex noise. Ear Hear 2016;37(3):312 – 23. http://dx.doi.org/10.1097/AUD.0000000000000251.
31. Zhao YM, Qiu W, Zeng L, Chen SS, Cheng XR, Davis RI, et al. Application of the kurtosis statistic to the evaluation of the risk of hearing loss in workers exposed to high-level complex noise. Ear Hear 2010;31(4):527 – 32. http://dx.doi.org/10.1097/AUD.0b013e3181d94e68.
32. Goley GS, Song WJ, Kim JH. Kurtosis corrected sound pressure level as a noise metric for risk assessment of occupational noises. J Acoust Soc Am 2011;129(3):1475 – 81. http://dx.doi.org/10.1121/1.3533691.

**Key Statistics**

National Center for Chronic and Noncommunicable Disease Control and Prevention

# Top 10 Causes of Death and the Most Growing Causes During the Chinese Spring Festival Holiday — China, 2017–2021

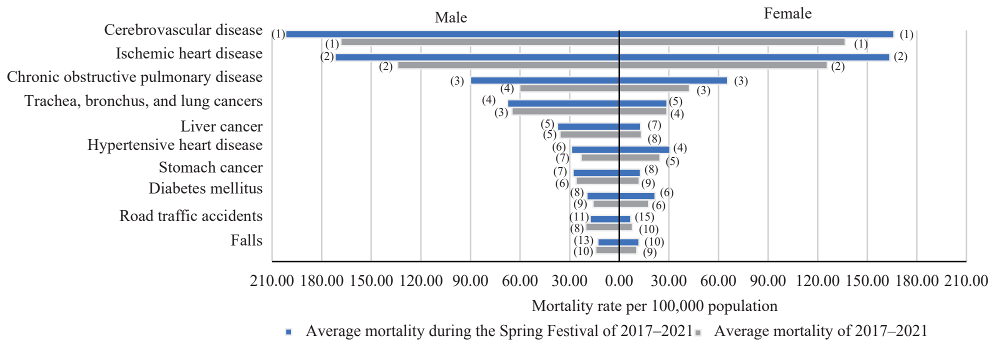


FIGURE 1. Comparison of the mortality rates of the top 10 leading causes of death* during the Chinese Spring Festival holiday†, § with the average annual mortality.

Note: The data tag indicates the ranking order of the disease among all causes of death.

* Causes of deaths are identified using the International Classification of Diseases, Tenth Revision (ICD-10) underlying cause of death codes.

† The Chinese Spring Festival holiday is defined as the seven-day public holiday occurring annually during the five-year period of 2017 to 2021.

§ Mortality rate during Chinese Spring Festival holiday is multiplied by 52 to compare it with the five-year average mortality rate.

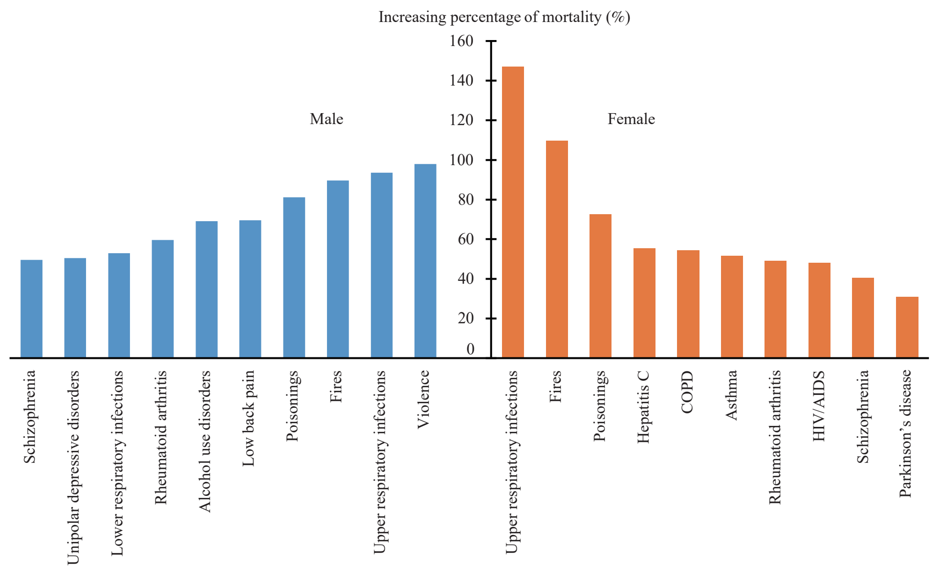


FIGURE 2. Top 10 diseases* with the highest percentage increase in mortality during the Chinese Spring Festival holiday†,§ compared with the average annual mortality.

* Causes of deaths are identified using the International Classification of Diseases, Tenth Revision (ICD-10) underlying cause of death codes.

† The Chinese Spring Festival holiday is defined as the seven-day public holiday occurring annually during the five-year period of 2017 to 2021.

§ Mortality rate during Chinese Spring Festival holiday is multiplied by 52 to compare it with the five-year average mortality rate.

Figure 1 shows the top 10 causes of death during the Spring Festival holidays from 2017 to 2021 and the 5-year average. The mortality rate during the Spring Festival holidays increased for cerebrovascular disease, ischemic heart disease, and chronic obstructive pulmonary disease (COPD) for both males and females. For males, the rankings of COPD, hypertensive heart disease, and diabetes increased, while the rankings of lung cancer and stomach cancer decreased. For females, the ranking of hypertensive heart disease increased, while the rankings of lung cancer, liver cancer, and stomach cancer decreased. These results suggest that more attention should be paid to patients with chronic diseases during the Spring Festival holiday.

Figure 2 shows the 10 diseases with the highest increase in mortality during the Chinese Spring Festival holiday compared with the five-year average. All changes in mortality were greater than 30%. The greatest increases in males were violence (98.02%), upper respiratory infections (93.60%), and fires (89.65%). The greatest increases in females were upper respiratory infections (147.11%), fires (109.73%), and poisonings (72.53%).

These results suggest that more attention should be paid to firework safety to reduce the occurrence of fire disasters. Additionally, the government should promote societal safety, as well as remind the public to have a healthy diet and drink in moderation during the festival.

**Source:** China Cause of Death Reporting System (CDRS), 2017–2021.

**Reported by:** Lin Lin; Jiangmei Liu, liujiangmei@ncncd.chinacdc.cn; Maigeng Zhou.

**doi:** 10.46234/ccdcw2023.013

Submitted: January 16, 2023; Accepted: January 18, 2023

Indexed by Science Citation Index Expanded (SCIE), Social Sciences Citation Index (SSCI), PubMed Central (PMC), Scopus, Chinese Scientific and Technical Papers and Citations, and Chinese Science Citation Database (CSCD)



The inauguration of *China CDC Weekly* is in part supported by Project for Enhancing International Impact of China STM Journals Category D (PIIJ2-D-04-(2018)) of China Association for Science and Technology (CAST).

CCDC weekly

*Vol. 5 No. 3 Jan. 20, 2023*

**Responsible Authority**

National Health Commission of the People's Republic of China

**Sponsor**

Chinese Center for Disease Control and Prevention

**Editing and Publishing**

China CDC Weekly Editorial Office
No.155 Changbai Road, Changping District, Beijing, China
Tel: 86-10-63150501, 63150701
Email: weekly@chinacdc.cn

**CSSN**

ISSN 2096-7071
CN 10-1629/R1